**Cell Culture** Human hepatocarcinoma HepG2 cells were obtained from the Japanese Cancer Research Resources Bank (Tokyo, Japan). The HepG2 cells and GnT-III gene transfectants were cultured in DMEM supplemented with 10% FCS and 0.1 mg/ml of ampicillin under a humidified atmosphere of 95% air and 5% $CO_2$. Following incubation for 1 d with serum-free DMEM, the cells were incubated with 50 ng/ml of HGF in serum-free DMEM.

**Expression Vector Construct, Gene Transfection, and Selection of Cells** The human GnT-III cDNA was amplified by PCR using human brain cDNA as a template. The cDNA fragment containing the entire coding sequence was inserted into the pCI-neo *EcoR* I site and the final construct, pCI-GnT-III, was obtained. The pCI-neo is a mammalian expression vector which includes the cytomegalovirus enhancer/promoter and the G418-resistant gene. HepG2 cells were plated in a 6-cm plastic culture dish at a density of $1\times10^6$ cells/ml. After 24 h, the cells were washed twice with ice-cold phosphate-buffered saline (PBS), pH 7.2, and the medium was changed to serum-free Opti-MEM. The pCI-GnT-III vector or pCI-neo vector (20 $\mu$g) was mixed with Lipofectamine plus, 100 $\mu$l of which was added to the HepG2 cells. After 5 h incubation, the medium was changed to DMEM supplemented with 10% FCS. Stable transfectants were selected using 1 mg/ml G418.

**GnT-III Activity** The GnT-III activity was measured according to the methods described previously.[11] Briefly, cell pellets were homogenized in ice-cold PBS containing protease inhibitors, and the supernatant was obtained after removal of the nucleus fraction by centrifugation for 20 min at $900\times g$. The GnT-III activity in the supernatant was assayed by high performance liquid chromatography methods using the fluorescence-labeled sugar chain (GlcNAc$\beta$-1, 2-Man$\alpha$-1, 6-[GlcNAc$\beta$-1, 2-Man$\alpha$-1, 3-] Man$\beta$-1, 4-GlcNAc$\beta$-1, 4-GlcNAc-pyridylamino) as a substrate. The substrate was prepared according to the method of Tokugawa *et al.*[12]

**Cell Scattering Assay** The HepG2 cells were plated in a 6-cm plastic culture dish at a density of $5\times10^4$ cells/ml. The HepG2 cells were allowed to grow as discrete colonies for 2—3 d. The culture medium was then replaced with fresh DMEM medium containing 50 ng/ml HGF. After 24 h, the cells were observed under a phase contrast microscope.

**Immunoprecipitation and Western Blot Analysis** The cultured cells were washed twice with ice-cold PBS and disrupted in the lysis buffer (20 mM Tris, pH 7.2, 1% Triton X-100, 10% glycerol, 1 mM APMSF, 5 mM aprotinin, 1 mM sodium orthovanadate, 10 mM sodium fluoride, and 10 mM iodoacetamide). The protein concentrations were determined using a protein assay kit (Bio-Rad, CA, U.S.A.). The cell-free lysates (1 mg) were immunoprecipitated with the anti-human c-Met antibody and protein G-immobilized magnetic beads (BioMag Protein G). For Western blot analysis, whole cell lysates or immunoprecipitates were subjected to 6 or 10% sodium dodecyl sulfate–polyacrylamide gel electrophoresis (SDS-PAGE) under reducing conditions, and then transferred to a PVDF membrane. The blot was blocked with 1% bovine serum albumin (BSA) in Tris-buffered saline containing 0.1% Tween 20 (TBST). For the detection of c-Met, the blot was incubated with anti-human c-Met antibody, and biotinylated anti-rabbit IgG antibody. For the detection of the phosphorylated tyrosine residues of c-Met, the blot was incubated with a monoclonal anti-phosphotyrosine antibody, and peroxidase-conjugated rabbit anti-mouse IgG. For the detection of phosphorylated ERK1/2, the blot was incubated with anti-ERK antibody, and biotinylated anti-mouse IgG antibody. Biotinylated antibody was detected using a Vectastain ABC-kit, and the blots were developed using the ECL chemiluminescence detection kit according to the manufacturer's instructions.

**Lectin Blot Analysis** Immunoprecipitated c-Met were subjected to 6% SDS-PAGE and transferred to PVDF membranes, as described above. The blot was blocked with 1% BSA in TBST and then incubated with 1 $\mu$g/ml biotinylated erythroagglutinating phytohemagglutinin (E-PHA) in TBST for 1 h at room temperature. After washing with TBST, the lectin-reactive proteins were detected using a Vectastain ABC kit and the ECL chemiluminescence detection kit.

## RESULTS

**Establishment of HepG2 Cell Lines Stably Expressing GnT-III** The GnT-III expression vector pCI-GnT-III was transfected into the HepG2 cells. The G418-resistant cells were screened as candidates of the GnT-III transfectants. Two randomly selected G418-resistant clones were evaluated for GnT-III activity. The clones expressing moderately and highly were designated HepG2-IIIm and HepG2-IIIh, respectively. A pCI-neo vector transfectant, designated as HepG2-mock, was also established as a negative control. The GnT-III activity in the HepG2-IIIm and HepG2-IIIh cells was significantly elevated about 20- and 250-fold, respectively, whereas the activity in the HepG2-mock cells did not differ significantly among the parental HepG2 cells (Table 1).

**Enhancement of HGF-Induced Cell Scattering in GnT-III Transfectants** To determine the effect of the overexpression of GnT-III on the HGF-induced cell scattering, the GnT-III transfectants and mock transfectants were examined. When the HepG2-mock cells were cultured, they showed a cobble-stone shape and had formed colonies of the cells (Fig. 1A). No significant difference in cell morphology of the GnT-III transfectants was observed (Figs. 1B, C). HepG2-mock cells scattered following cell-cell dissociation by the stimulation with HGF (Fig. 1D). The cell scattering of the GnT-III transfectants was more pronounced than the HepG2-mock cells; the enhancement of cell scattering was most pronounced in the HepG2-IIIh cells that had a high GnT-III activity (Figs. 1E, F).

**Analysis of c-Met of GnT-III Transfectants** The expression levels of the c-Met protein in GnT-III transfectants were analyzed by Western blot analysis. No significant change of the level of c-Met was observed (Fig. 2). To analyze the alterations of the *N*-glycan structure on c-Met, E-

Table 1. Enzyme Activities of GnT-III in Mock- and GnT-III Transfected HepG2 Cells

| Cell line | GnT-III activity [pmol/h/mg protein] |
|---|---|
| HepG2 | 79±30 |
| HepG2-mock | 149±50 |
| HepG2-IIIm | 1400±260 |
| HepG2-IIIh | 19600±1350 |

Data were mean±S.E. of three separate experiments.

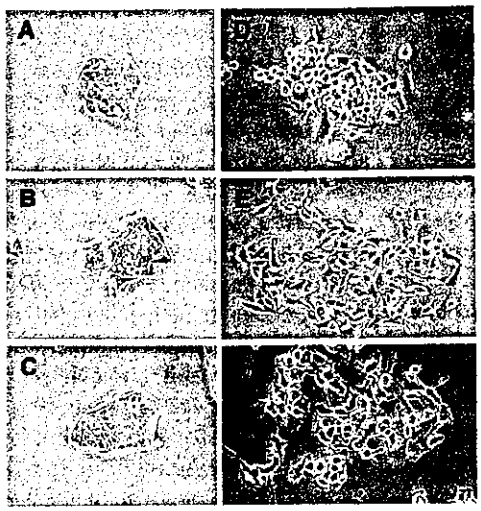


Fig. 1. HGF-Induced Cell Scattering in HepG2-Mock Cells and GnT-III Transfected HepG2 Cells

HepG2 mock-cells (A, D), HepG2-IIIm cells (B, E), and HepG2-IIIh cells (C, F) were cultured with (D, E, F) or without (A, B, C) HGF (50 ng/ml) for 24 h. Representative fields were photographed using a phase-contrast microscope.

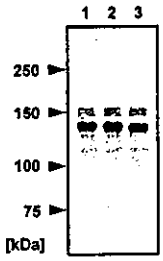


Fig. 2. Western Blot Analysis of c-Met

Total cell lysates from HepG2-mock cells (lane 1), HepG2-IIIm cells (lane 2), and HepG2-IIIh cells (lane 3) were subjected to 6% SDS-PAGE and then transferred to PVDF membrane. The blots were probed with anti-c-Met antibody.

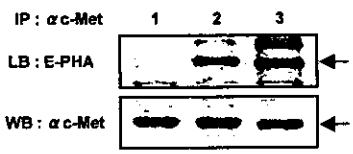


Fig. 3. Lectin Blot Analysis of c-Met

C-Met was immunoprecipitated from cell lysates of HepG2-mock cells (lane 1), HepG2-IIIm cells (lane 2), and HepG2-IIIh cells (lane 3). Immunoprecipitates were subjected to 6% SDS-PAGE and then transferred to PVDF membrane. The blots were probed with E-PHA (upper panel) or anti-c-Met antibody (lower panel). Arrows indicate c-Met.

PHA lectin blot analysis was performed. E-PHA binds specifically to bisecting GlcNAc residues.[13] Immunoprecipitated c-Met from the HepG2-IIIm cells and the HepG2-IIIh cells showed significant reactivity of E-PHA (Fig. 3), showing that *N*-glycan on c-Met was modified with bisecting GlcNAc residues. It was noted that the apparent molecular size of c-Met from the HepG2-IIIh cells were smaller than that from the HepG2-mock cells. The following experiments were performed with HepG2-IIIh cells and HepG2-mock cells.

**Tyrosine Phosphorylation of c-Met in Gn T-III Transfectants** To determine the effect of the GnT-III transfection on HGF signaling, HGF-induced tyrosine phosphorylation of

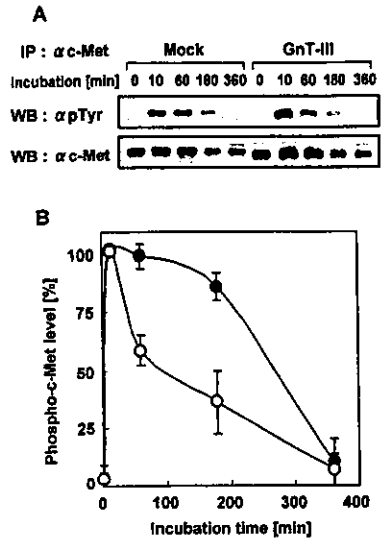


Fig. 4. The Time Course of the Tyrosine Phosphorylation of c-Met

(A) Cells were harvested at the indicated time after HGF treatment (50 ng/ml). C-Met, immunoprecipitated from the cell lysates of HepG2-mock cells (●) and HepG2-IIIh cells (○) were subjected to 6% SDS-PAGE and then transferred to a PVDF membrane. The blot was probed with anti-phosphotyrosine antibody (upper panel) or anti-human c-Met antibody (lower panel). One representative result of three separate experiments is shown. (B) The intensities of the bands obtained with phosphorylated c-Met were normalized to the intensities of the c-Met bands. These values are shown as percentages of the level of c-Met phosphorylation in HepG2-mock cells treated with HGF for 10 min (mean±S.E., three separate experiments).

c-Met in HepG2-IIIh cells and HepG2-mock cells were examined. The c-Met phosphorylation level reached a peak by 10 min after the HGF treatment in each transfectant. Although no difference in the peak level of c-Met phosphorylation between the HepG2-IIIh cells and HepG2-mock cells was observed, the level of c-Met phosphorylation in the HepG2-IIIh cells was reduced more rapidly than in the HepG2-mock cells (Fig. 4).

**ERK Activation in GnT-III Transfectants** To further clarify the effect of the GnT-III transfection on HGF signaling, the HGF-induced phosphorylation of ERK in the HepG2-IIIh cells and HepG2-mock cells was also examined. The time course of the tyrosine phosphorylation of ERK showed that the phosphorylated ERK level reached a peak by 10 min after treatment in each transfectant. The peak level in the HepG2-IIIh cells was slightly higher than in the HepG2-mock cells (Fig. 5).

## DISCUSSION

In this paper we investigated the effects of the overexpression of GnT-III on the scattering of human hepatocarcinoma HepG2 cells, a defined HGF-induced biological response, since the function of the HGF receptor c-Met could be modulated by GnT-III transfection followed by the alteration of its biological functions, as described in the "INTRODUCTION" section. The results showed that GnT-III gene transfection increases GnT-III activity by about 250 fold, followed by a significant increase of E-PHA reactivity with c-Met (Fig. 3), indicating that the transfection of GnT-III increased the amount of bisecting oligosaccharide residue on c-Met. In addition, the molecular size of c-Met in the HepG2-IIIh cells was smaller than that in the HepG2-mock cells (Figs. 2, 3), suggesting that an elongation of *N*-glycans on c-Met was

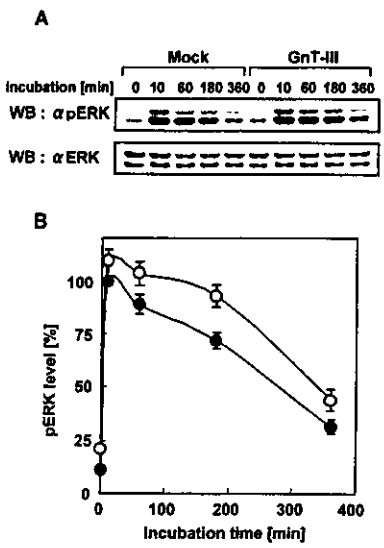


Fig. 5. The Time-Course of the Tyrosine Phosphorylation of ERK

(A) Cells were stimulated with 50 ng/ml HGF and harvested at the indicated times. Whole cell lysates of HepG2-mock cells (●) and HepG2-IIIh cells (○) were subjected to 10% SDS-PAGE and then transferred to a PVDF membrane. The blot was probed with anti-phospho-ERK antibody (upper panel) or anti-ERK antibody (lower panel). One representative result of three separate experiments is shown. (B) The intensities of the bands obtained with phospho-ERK were normalized to the intensities of the ERK bands. These values are shown as percentages of the level of ERK phosphorylation in HepG2-mock cells treated with HGF for 10 min (mean±S.E., three separate experiments).

suppressed by the bisecting GlcNAc residue. The same observation has been shown in various glycoproteins such as the EGF receptor,[7] E-cadherin,[14,15] and CD44.[16]

We investigated the effect of the overexpression of GnT-III on HGF-induced cell scattering using these transfectants, because cell scattering is one of the HGF-induced biological responses and an important component of several physiological and pathological processes. We found that HGF-induced cell scattering in the GnT-III transfectants was enhanced depending on the GnT-III activities. As far as we know, this is the first report of the enhancing effect of HGF-induced cell scattering by the overexpression of GnT-III.

To confirm the effect of GnT-III overexpression on HGF signaling, we first investigated the effect on the HGF-induced tyrosine phosphorylation of c-Met in GnT-III transfectants. Unexpectedly, the peak level of the tyrosine phosphorylation of c-Met did not change by GnT-III. In addition, the level of c-Met phosphorylation was reduced quite a bit more rapidly than that in the HepG2-mock cells. Previous studies shown that HGF stimulation also leads to down-regulation of the receptor.[17] We assume that the rapid dephosphorylation was caused by up-regulated HGF signaling.

We further examined the effects on the HGF-induced phosphorylation of ERK, because ERK activation is associated with HGF-induced cell scattering.[18] The ERK phosphorylation was slightly enhanced by the GnT-III overexpression, showing that the enhancement of cell scattering involves the up-regulation of the HGF-induced ERK phosphorylation. The mechanisms by which GnT-III overexpression affects ERK activation is now under investigation. It has been shown that GnT-III overexpression enhances the EGF-induced ERK phosphorylation in HelaS3 cells by up-regulation of the internalization rate of the receptors.[7] A possible mechanism by which GnT-III overexpression enhances HGF-induced ERK phosphorylation is that GnT-III affects c-Met internalization.

In this study, we demonstrated that GnT-III overexpression increased the amount of bisecting oligosaccharide structures and shortened the *N*-glycans associated with c-Met. Lectin blot analysis of total showed that *N*-glycans of the other glycoproteins were also changed by GnT-III overexpression (data not shown). Therefore, the glycoproteins involved in cell scattering, such as E-cadherin and integrin, are candidate proteins for involvement in the enhancement of cell scattering by GnT-III overexpression. In fact, it has been reported that GnT-III overexpression affects their biological functions.[14,15,19] Further study is needed to clarify the mechanism involved in the enhancement of cell scattering.

In evaluating the significance of the present results, it seems worthwhile to examine the relation of the change of GnT-III with the action of HGF *in vivo*. In the normal rat liver, GnT-III activity is very low. However, the activity increased about 4-fold in regenerating rat liver.[9] HGF is induced in regenerating rat liver, and stimulates hepatocyte growth. In addition, it was shown that hepatocarcinoma exhibited a high level of GnT-III activity, whereas normal liver contains very little.[20] Autocrine HGF signaling leads to abnormal malignant progression.[21] Therefore, the increase of GnT-III may contribute to liver regeneration and hepatocarcinoma progression by the enhanced HGF signal.

In conclusion, we demonstrated that the overexpression of GnT-III caused the enhancement of HGF-induced cell scattering, and suggest that the enhancement of cell scattering involves, at least in part, enhancement of the HGF-induced ERK phosphorylation.

**Acknowledgments** This work was supported by a grant-in-aid for research on health sciences focusing on drug innovation from the Japan Health Sciences Foundation.

## REFERENCES

1) Nishikawa A., Ihara Y., Hatakeyama M., Kangawa K., Taniguchi N., *J. Biol. Chem.*, **267**, 18199—18204 (1992).
2) Easton E. W., Bolscher J. G., van den Eijnden D. H., *J. Biol. Chem.*, **266**, 21674—21680 (1991).
3) Gu J., Nishikawa A., Tsuruoka N., Ohno M., Yamaguchi N., Kangawa K., Taniguchi N., *J. Biochem.* (Tokyo), **113**, 614—619 (1993).
4) Sasai K., Ikeda Y., Eguchi H., Tsuda T., Honke K., Taniguchi N., *FEBS Lett.*, **522**, 151—155 (2002).
5) Stanley P., *Biochim. Biophys. Acta*, **1573**, 363—368 (2002).
6) Rebbaa A., Yamamoto H., Saito T., Meuillet E., Kim P., Kersey D. S., Bremer E. G., Taniguchi N., Moskal J. R., *J. Biol. Chem.*, **272**, 9275—9279 (1997).
7) Sato Y., Takahashi M., Shibukawa Y., Jain S. K., Hamaoka R., Miyagawa J., Yaginuma Y., Honke K., Ishikawa M., Taniguchi N., *J. Biol. Chem.*, **276**, 11956—11962 (2001).
8) Ihara Y., Sakamoto Y., Mihara M., Shimizu K., Taniguchi N., *J. Biol. Chem.*, **272**, 9629—9634 (1997).
9) Miyoshi E., Ihara Y., Nishikawa A., Saito H., Uozumi N., Hayashi N., Fusamoto H., Kamada T., Taniguchi N., *Hepatology*, **22**, 1847—1855 (1995).
10) Miyoshi E., Nishikawa A., Ihara Y., Gu J., Sugiyama T., Hayashi N., Fusamoto H., Kamada T., Taniguchi N., *Cancer Res.*, **53**, 3899—3902 (1993).
11) Nishikawa A., Fujii S., Sugiyama T., Taniguchi N., *Anal. Biochem.*, **170**, 349—354 (1988).
12) Tokugawa K., Oguri S., Takeuchi M., *Glycoconj. J.*, **13**, 53—56 (1996).
13) Yamashita K., Hitoi A., Kobata A., *J. Biol. Chem.*, **258**, 14753—14755

(1983).
14) Yoshimura M., Ihara Y., Matsuzawa Y., Taniguchi N., *J. Biol. Chem.*, **271**, 13811—13815 (1996).
15) Kitada T., Miyoshi E., Noda K., Higashiyama S., Ihara H., Matsuura N., Hayashi N., Kawata S., Matsuzawa Y., Taniguchi N., *J. Biol. Chem.*, **276**, 475—480 (2001).
16) Sheng Y., Yoshimura M., Inoue S., Oritani K., Nishiura T., Yoshida H., Ogawa M., Okajima Y., Matsuzawa Y., Taniguchi N., *Int. J. Cancer*, **73**, 850—858 (1997).
17) Hammond D. E., Carter S., McCullough J., Urbe S., Vande Woude G., Clague M. J., *Mol. Biol. Cell.*, **14**, 1346—1354 (2001).
18) Sipeki S., BanderE., Buday L., Farkas G., Bacsy E., Ways D. K., Farago A., *Cell Signal*, **11**, 885—890 (1999).
19) Isaji T., Gu J., Nishiuchi R., Zhao Y., Takahashi M., Miyoshi E., Honke K., Sekiguchi K., Taniguchi N., *J. Biol. Chem.*, in press (2004).
20) Nishikawa A., Fujii S., Sugiyama T., Hayashi N., Taniguchi N., *Biochem. Biophys. Res. Commun.*, **152**, 107—112 (1988).
21) Vande Woude G. F., Jeffers M., Cortner J., Alvord G., Tsarfaty I., Resau J., *Ciba Found. Symp.*, **212**, 119—130; discussion 130—112, 148—154 (1997).

Original Paper

International Archives of Allergy and Immunology

Int Arch Allergy Immunol 2005;136:23–32
DOI: 10.1159/000082581

Received: April 27, 2004
Accepted after revision: September 1, 2004
Published online: December 8, 2004

# Kinetic Analysis of Pepsin Digestion of Chicken Egg White Ovomucoid and Allergenic Potential of Pepsin Fragments

Kayoko Takagi[a] Reiko Teshima[a] Haruyo Okunuki[a] Satsuki Itoh[a]
Nana Kawasaki[a] Toru Kawanishi[a] Takao Hayakawa[a] Yoichi Kohno[b]
Atsuo Urisu[c] Jun-ichi Sawada[a]

[a]National Institute of Health Sciences, Tokyo; [b]Department of Pediatrics, Graduate School of Medicine, Chiba University, Chiba, and [c]Department of Pediatrics, Fujita Health University School of Medicine, Aichi, Japan

**Key Words**
Ovomucoid · Allergen · Digestion · Simulated gastric fluid · Fragment, pepsin-digested · Human serum IgE

**Abstract**
***Background:*** The allergenic potential of chicken egg white ovomucoid (OVM) is thought to depend on its stability to heat treatment and digestion. Pepsin-digested fragments have been speculated to continue to exert an allergenic potential. OVM was digested in simulated gastric fluid (SGF) to examine the reactivity of the resulting fragments to IgE in sera from allergic patients. ***Methods:*** OVM was digested in SGF and subjected to SDS-PAGE. The detected fragments were then subjected to N-terminal sequencing and liquid chromatography/mass spectrometry/mass spectrometry analysis to confirm the cleavage sites and partial amino acid sequences. The reactivity of the fragments to IgE antibodies in serum samples from patients allergic to egg white was then determined using Western blotting (n = 24). ***Results:*** The rate of OVM digestion depended on the pepsin/OVM ratio in the SGF. OVM was first cleaved near the end of the first domain, and the resulting fragments were then further digested into smaller fragments. In the Western blot analysis, 93% of the OVM-reactive sera also bound to the 23.5- to 28.5-kDa fragments, and 21% reacted with the smaller 7- and 4.5-kDa fragments. ***Conclusion:*** When the digestion of OVM in SGF was kinetically analyzed, 21% of the examined patients retained their IgE-binding capacity to the small 4.5-kDa fragment. Patients with a positive reaction to this small peptide fragment were thought to be unlikely to outgrow their egg white allergy. The combination of SGF-digestibility studies and human IgE-binding experiments seems to be useful for the elucidation and diagnosis of the allergenic potential of OVM.



## Introduction

Chicken egg white is one of the strongest and most frequent causes of food allergies among young children [1–5]. Egg white contains several allergens, including ovalbumin, ovotransferrin, lysozyme and ovomucoid (Gal d 1, OVM). OVM accounts for about 11% of all egg white proteins [6] and has a molecular weight of 28 kDa, containing a carbohydrate content of 20–25% [7]. OVM is known to be stable to digestion and heat, and cooked eggs can cause allergic reactions in OVM-specific allergic patients [8–11]. One possible reason for this is that OVM contains linear epitopes that are only slightly affected by conformational changes induced by heat denaturation.

KARGER
Fax + 41 61 306 12 34
E-Mail karger@karger.ch
www.karger.com


1018–2438/05/1361–0023$22.00/0

Accessible online at:
www.karger.com/iaa

Correspondence to: Dr. Reiko Teshima
National Institute of Health Sciences, Division of Biochemistry and Immunochemistry
1-18-1 Kamiyoga, Setagaya-ku
Tokyo 158-8501 (Japan)
Tel. +81 3 3700 1141, ext. 243, Fax +81 3 3707 6950, E-Mail rteshima@nihs.go.jp

OVM consists of 186 amino acids divided into three domains of about 60 amino acids each; the third domain has been reported to be the most important domain with regard to allergenicity [12]. In a previous report, N-glycans in the third domain were suggested to be essential for allergenicity [13]; however, a recent report found that the deletion of the N-glycans did not affect the allergic reactivity.

We previously reported the digestibility of 10 kinds of food proteins in simulated gastric fluid (SGF) [8, 14]. OVM was digested relatively rapidly, but several fragments were detected by sodium dodecyl sulfate-polyacrylamide gel electrophoresis (SDS-PAGE) followed by Coomassie blue (CBB) staining. The reactivity of these fragments with IgE antibodies from the sera of patients with egg white allergy is very important to understanding the mechanism of OVM allergy.

A few previous reports have described the reactivity of IgE in sera from patients with egg white allergies with OVM-derived fragments. Kovacs-Nolan et al. [15] separated pepsin-digested fragments of OVM using high-performance liquid chromatography (HPLC) and examined the IgE-binding activities of each fragment using an enzyme-linked immunosorbent assay (ELISA). Besler et al. [16] investigated the reactivity of pepsin-digested fragments with patient IgE using Western blotting and showed that the fragments retain their binding capacity to human IgE in some serum samples from OVM-allergic patients. However, little attention has been paid to the digestive conditions, and the number of serum samples has been somewhat small in these studies. Urisu et al. [17] reported that the sera of subjects that tested positive or negative during an oral egg white challenge exhibited a significant difference in their reactivity with pepsin fragments.

In the present report, kinetic data for different generations of SGF-stable OVM fragments were obtained, and the reactivity of the fragments with serum IgE from patients with egg white allergies was investigated using Western blotting.

## Materials and Methods

Pepsin (catalog number P6887) and chicken egg white OVM (T2011, Trypsin Inhibitor, Type III-O) were purchased from Sigma Chemical Co. (St. Louis, Mo., USA). The concentration of the OVM test solution was 5 mg/ml of water. The gels and reagents used for the SDS-PAGE analysis were purchased from Invitrogen (Carlsbad, Calif., USA).

*Serum Specimens*

Sera from 24 patients with egg white allergies and a healthy volunteer were used after obtaining informed consent from the patients and ethical approval by the Institutional Review Board of the National Institute of Health Sciences. Twenty-two of the patients had been diagnosed as having an egg white allergy at hospitals in Japan, based on their clinical histories and positive IgE responses to egg white proteins by radioallergosorbent test (RAST), while the remaining 2 allergen-specific sera were purchased from Plasma Lab International (Everett, Wash., USA); the commercial sera originated from adult Caucasians who had been diagnosed as having several food allergies, including egg white, based on their clinical history and skin tests. The commercial sera also showed positive IgE responses to egg white proteins when examined using RAST.

*Preparation of SGF*

Pepsin (3.8 mg; approximately 13,148 units of activity) was dissolved in 5 ml of gastric control solution (G-con; 2 mg/ml NaCl, pH adjusted to 2.0 with distilled HCl), and the activity of each newly prepared SGF solution was defined as the production of a $\Delta A280$ of 0.001/min at pH 2.0 and 37°C, measured as the production of trichloroacetic acid-soluble products using hemoglobin as a substrate. The original SGF was prepared at a pepsin/OVM concentration of 10 unit/μg, and this solution was diluted with G-con for the experiments performed at pepsin/OVM concentrations of 1 and 0.1 unit/μg. The SGF solutions were used within the same day.

*Digestion in SGF*

SGF (1,520 μl) was incubated at 37°C for 2 min before the addition of 80 μl of OVM solution (5 mg/ml). The digestion was started by the addition of OVM. At each scheduled time point (0.5, 2, 5, 10, 20, 30, and 60 min), 200 μl of the reaction mixture was transferred to a sampling tube containing 70 μl of 5× Laemmli buffer (40% glycerol, 5% 2-mercaptoethanol, 10% SDS, 0.33 *M* Tris, 0.05% bromophenol blue, pH 6.8) and 70 μl of 200 m*M* $Na_2CO_3$. For the zero-point samples, the OVM solution (10 μl) was added to neutralized SGF (190 μl of SGF, 70 μl of 5× Laemmli buffer, and 70 μl of 200 m*M* $Na_2CO_3$). All neutralized samples were then boiled at 100°C for 3 min and subjected to SDS-PAGE.

*SDS-PAGE Analysis and Staining Procedure*

Samples (15 μl/lane) were loaded onto a 10–20% polyacrylamide Tris/Tricine gel (Invitrogen, Carlsbad, Calif., USA) and separated electrophoretically. The gels were fixed for 5 min in 5% trichloroacetic acid, washed for 2 h with SDS Wash (45.5% methanol, 9% acetic acid), stained for 10 min with CBB solution (0.1% Coomassie Brilliant blue R, 15% methanol, 10% acetic acid), and destained with 25% methanol and 7.5% acetic acid. The stained gel images were then analyzed using Image Gauge V3.1 (Fuji Film, Tokyo, Japan), and the density of each band was quantified. Periodic acid-Schiff (PAS) staining [18] was used to detect the glycosylated fragments.

*N-Terminal Sequence Analysis*

OVM (1.5 mg) was digested in SGF containing 1 unit/ml pepsin, concentrated by centrifugation using Centriprep YM-3 (Millipore Corporation, Bedford, Mass., USA) and subjected to SDS-PAGE followed by electrical transblotting to a 0.2-μm polyvinylidene difluoride membrane (Bio-Rad, Richmond, Calif., USA) and CBB staining. The detected fragment bands were then cut out and sequenced using a Procise 494HT Protein Sequencing System (Applied Biosys-

tems, Foster City, Calif., USA) or an HP G1005A Protein Sequencing System (Hewlett-Packard, Palo Alto, Calif., USA); each fragment was analyzed for 5 cycles.

*Carboxymethylation and Peptide Mapping Using Liquid Chromatography/Mass Spectrometry/Mass Spectrometry (LC/MS/MS)*

The digested OVM sample was separated electrophoretically as described above, stained with CBB, and the stained bands were cut out. The gel pieces were homogenized in 20 m*M* Tris-HCl (pH 8.0) containing 0.1% SDS and the proteins were extracted. The extracts were concentrated and purified by acetone precipitation. The acetone precipitates were incubated with 2-mercaptethanol (92.5 m*M*) in 72 µl of 0.5 *M* Tris-HCl buffer (pH 8.6) containing 8 *M* guanidine hydrochloride and 5 m*M* EDTA at room temperature for 2 h. To this solution, 1.5 mg of monoiodoacetic acid was added, and the mixture was incubated at room temperature for 2 h in the dark. The reaction mixture was desalted using a MicroSpin G-25 column (Amersham Bioscience, Uppsala, Sweden) and lyophilized. Reduced and carboxymethylated proteins were digested with trypsin (50 ng/µl in 50 m*M* $NH_4HCO_3$).

Tandem electrospray mass spectra were recorded using a hybrid quadruple/time-of-flight spectrometer (Qstar Pulsar i; Applied Biosystems, Foster City, Calif., USA) interfaced to a CapLC (Magic 2002; Michrom BioResources, Auburn, Calif., USA). Samples were dissolved in water and injected into a C18 column (0.2 × 50 mm, 3 µm, Magic C18, Michrom BioResources). Peptides were eluted with a 5–36% acetonitrile gradient in 0.1% aqueous formic acid over 60 min at a flow rate of 1 µl/min after elution with 5% acetonitrile for 10 min. The capillary voltage was set to 2,600 V, and data-dependent MS/MS acquisitions were performed using precursors with charge states of 2 and 3 over a mass range of 400–2,000.

*Western Blotting of Digested Fragments with Human Serum IgE*

The digested OVM samples were applied to a 10–20% polyacrylamide Tris/Tricine 2D gel, followed by electrical transfer to a nitrocellulose membrane. The membrane was then blocked with 0.5% casein-PBS (pH 7.0) and cut into 4-mm strips. The strips were incubated with diluted human serum (1/4 to 1/5) in 0.2% casein-PBS (pH 7.0) at room temperature for 1 h and then at 4°C for 18 h. After washing with 0.05% Tween 20-PBS, the strips were incubated with rabbit anti-human IgE (Fc) antibodies (Nordic Immunological Laboratories, Tilburg, The Netherlands) at room temperature for 1 h, and then with horseradish peroxidase-conjugated donkey anti-rabbit Ig antibodies (Amersham Biosciences, Little Chalfont, UK) at room temperature for 1 h. Finally, the strips were reacted with Konica ImmunoStain HRP-1000 (Konica, Tokyo, Japan), according to the manufacturer's protocol.

## Results

*Kinetics of OVM Digestion by Pepsin*

OVM was digested in SGF containing various concentrations of pepsin, and the fragments were separated by SDS-PAGE and stained with CBB (fig. 1). The molecular weight of OVM, based on its amino acid sequence, is about 20 kDa, but a broad band representing intact OVM appeared at about 34–49 kDa in the SDS-PAGE gel because of the presence of five N-linked sugar chains. The pepsin band was detected at 39 kDa, overlapping with the intact OVM band, and lysozyme (14 kDa) contamination was detected in the OVM sample that was used. Intact OVM rapidly disappeared within 0.5 min in SGF (pepsin/OVM = 10 unit/µg), and a fragment band was detected at 7 kDa. When the pepsin content in SGF was reduced to 1 and 0.1 unit/µg, the digestion rate markedly decreased. Intact OVM was still detected after 30 min when the pepsin/OVM ratio was 0.1 unit/µg. The fragment bands were clearer (fig. 2) when a concentrated SGF-digested OVM solution (pepsin/OVM = 1 unit/µg, digestion times 5 and 30 min) was used, followed by SDS-PAGE. As shown in figure 2, a strong 23.5- to 28.5-kDa band (FR 1) was detected at 5 min, while 10- (FR 2), 7- (FR 3) and 4.5- to 6-kDa (FR 4) bands were detected after 30 min. FR 1 and FR 2 were both positively stained by PAS, suggesting that the FR 1 and FR 2 fragments have high carbohydrate contents. The time courses for the amounts of intact OVM and the four fractions are plotted in figure 3, where the pepsin/OVM ratio is 1 unit/µg. FR 1 rapidly increased but slowly disappeared after 2 min. FR 2 and FR 3 also rapidly reached maximum values at 5 min and then slowly disappeared. On the other hand, FR 4 gradually increased throughout the entire period of the experiment.

Preheating (at 100°C for 5 or 30 min) of the OVM solution (5 mg/ml in water) did not influence the digestion pattern (fig. 1).

**Table 1.** N-Terminal sequences of pepsin fragments

| Digestion period | Fraction | Fragment | Residues | Sequence | Ratio %[a] |
|---|---|---|---|---|---|
| 5 min | FR 1 | 1-1 | 50–54 | FGTNI | 73.1 |
| | | 1-2 | 51–55 | GTNIS | 11.6 |
| | | 1-3 | 1–5 | AEVDC | 6.9 |
| 5 min | FR 2 | 2-1 | 1–5 | AEVDC | 68.8 |
| | | 2-2 | 134–138 | VSVDC | 28.2 |
| 5 min | FR 3 | 3-1 | 1–5 | AEVDC | 48.4 |
| | | 3-2 | 134–138 | VSVDC | 24.3 |
| | | 3-3 | 104–108 | NECLL | 9.6 |
| | | 3-4 | 85–89 | VLCNR | 6.5 |
| 30 min | FR 4 | 4-1 | 134–138 | VSVDC | 30.6 |
| | | 4-2 | 104–108 | NECLL | 24.0 |
| | | 4-3 | 19–23 | VLVCN | 20.6 |

[a] Molar ratios of the fragments to the total amount in each fraction.

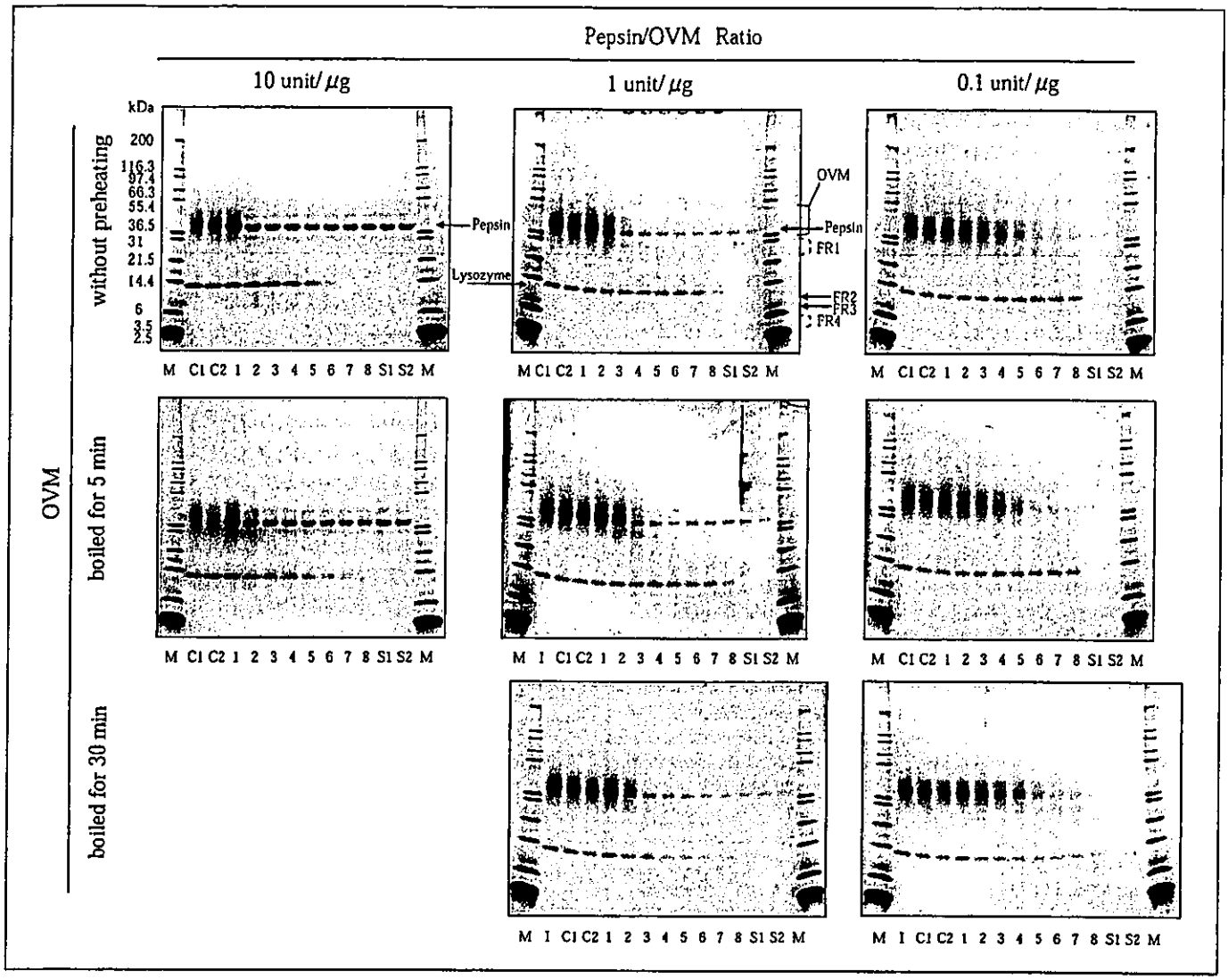


**Fig. 1.** Kinetic patterns of OVM digestion in SGF-containing pepsin. Digested samples were analyzed by SDS-PAGE followed by CBB staining. The digestion patterns of OVM without preheating (upper panels), preheated at 100°C for 5 min (middle panels), and preheated at 100°C for 30 min (lower panels) are shown. The ratio of pepsin to OVM was 10 unit/1 μg (left), 1 unit/1 μg (middle), and 0.1 unit/1 μg (right). Lane M = Molecular weight markers; lanes C1 and C2 = OVM without pepsin at 0 (C1) and 60 (C2) min; lanes 1–8 = SGF-digested OVM at 0, 0.5, 2, 5, 10, 20, 30 and 60 min, respectively; lanes S1 and S2 = SGF alone at 0 (S1) and 60 (S2) min; lanes I = OVM without preheating; FR 1 = fraction 1 containing a fragment at 23.5–28.5 kDa; FR 2 = fraction 2 containing a 10-kDa fragment; FR 3 = fraction 3 containing a 7-kDa fragment; FR 4 = fraction 4 containing 4.5- to 6-kDa fragments.

*Sequence Analysis of OVM Fragments*

The sequences of the five N-terminal residues in each fragment were analyzed, and the data are summarized in table 1. Figure 4 schematically depicts the identified fragments; the arrows in the upper panel indicate the sites of pepsin cleavage.

The internal sequences of the FR 1, FR 3, and FR 4 fragments were also identified by LC/MS/MS and are shown in table 2 and in the upper panel of figure 4.

*Reactivity of the Fragments with Serum IgE from Patients with Egg White Allergy*

Western blot analysis using patient sera as the source of the primary antibodies was performed to identify sera that reacted with intact OVM and the SGF fragments. Representative blotting data are shown in figure 5, and all the results are listed in table 3. Ninety-two percent of the serum samples from allergic patients reacted with OVM, and 93% of the OVM-positive sera reacted with FR 1

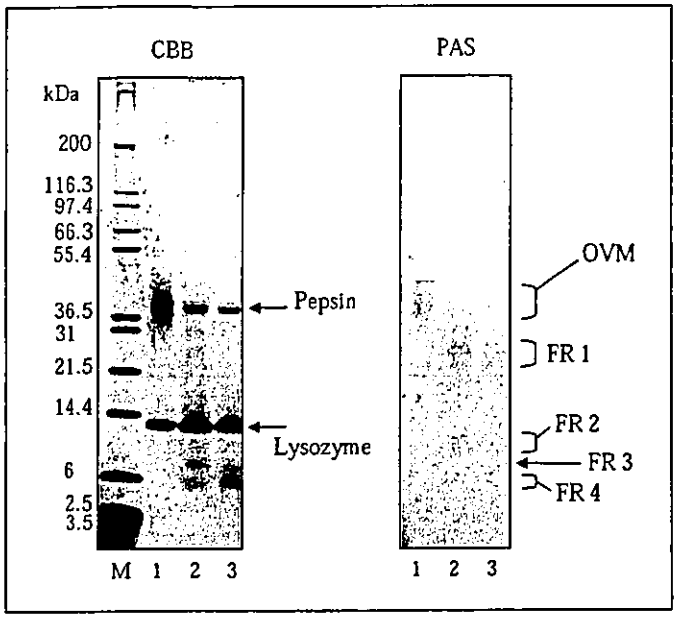


**Fig. 2.** CBB and PAS staining of OVM fragments following digestion in SGF (pepsin/OVM = 1 unit/μg) for 5 and 30 min. Lane M = Molecular weight markers; lane 1 = original OVM (2.5 μg/lane); lanes 2 and 3 = OVM digested for 5 and 30 min, respectively, and concentrated (12 μg, equivalent to the original OVM/lane). Samples were applied to two SDS-PAGE gels and electrophoresed. One plate (left panel) was stained with CBB reagent, and the other (right panel) was stained with PAS reagent.

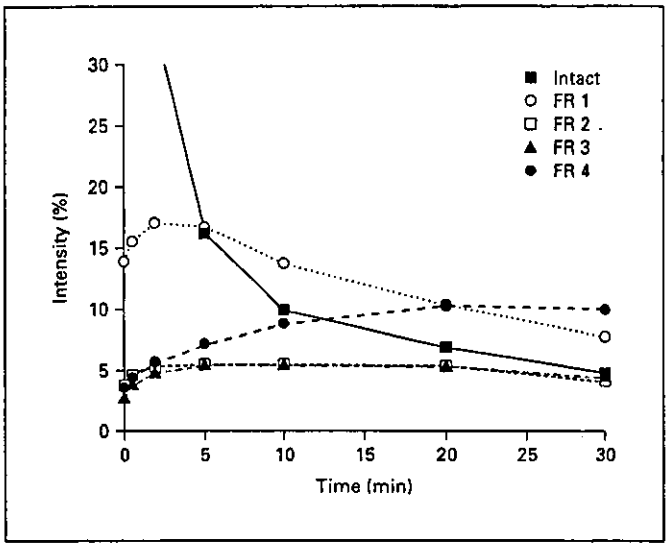


**Fig. 3.** Quantification of the SGF-digestion pattern of intact OVM and the digestion fragments at a pepsin/OVM ratio of 1 unit/μg. The intensity of each band was calculated using the ratio of the band's density to the total density of the originally detected band at t = 0. Values are the mean of duplicate analyses. Similar results were observed in another set of experiments.

**Table 2.** Identified inside sequences in pepsin- and trypsin-digested OVM

| Pepsin digestion | Fraction | Residues | Sequence |
|---|---|---|---|
| 5 min | FR 1 | 83–89 | VMVLCNR |
| | | 90–103 | AFNPVCGTDGVTYD |
| | | 90–112 | AFNPVCGTDGVTYDNECLLCAHK |
| | | 90–122 | AFNPVCGTDGVTYDNECLLCAHKVEQGASVDKR |
| | | 113–122 | VEQGASVDKR |
| 5 min | FR 3 | 90–112 | AFNPVCGTDGVTYDNECLLCAHK |
| | | 90–122 | AFNPVCGTDGVTYDNECLLCAHKVEQGASVDKR |
| | | 104–111 | NECLLCAH |
| | | 104–112 | NECLLCAHK |
| | | 104–121 | NECLLCAHKVEQGASVDK |
| | | 104–122 | NECLLCAHKVEQGASVDKR |
| | | 113–122 | VEQGASVDKR |
| | | 134–159 | VSVDCSEYPKPDCTAEDRPLCGSDNK |
| | | 165–185 | CNFCNAVVESNGTLTLSHFGK |
| 30 min | FR 4 | 90–112 | AFNPVCGTDGVTYDNECLLCAHK |
| | | 104–111 | NECLLCAH |
| | | 104–112 | NECLLCAHK |
| | | 104–122 | NECLLCAHKVEQGASVDKR |
| | | 112–122 | KVEQGASVDKR |
| | | 113–121 | VEQGASVDK |
| | | 113–122 | VEQGASVDKR |
| | | 165–185 | CNFCNAVVESNGTLTLSHFGK |

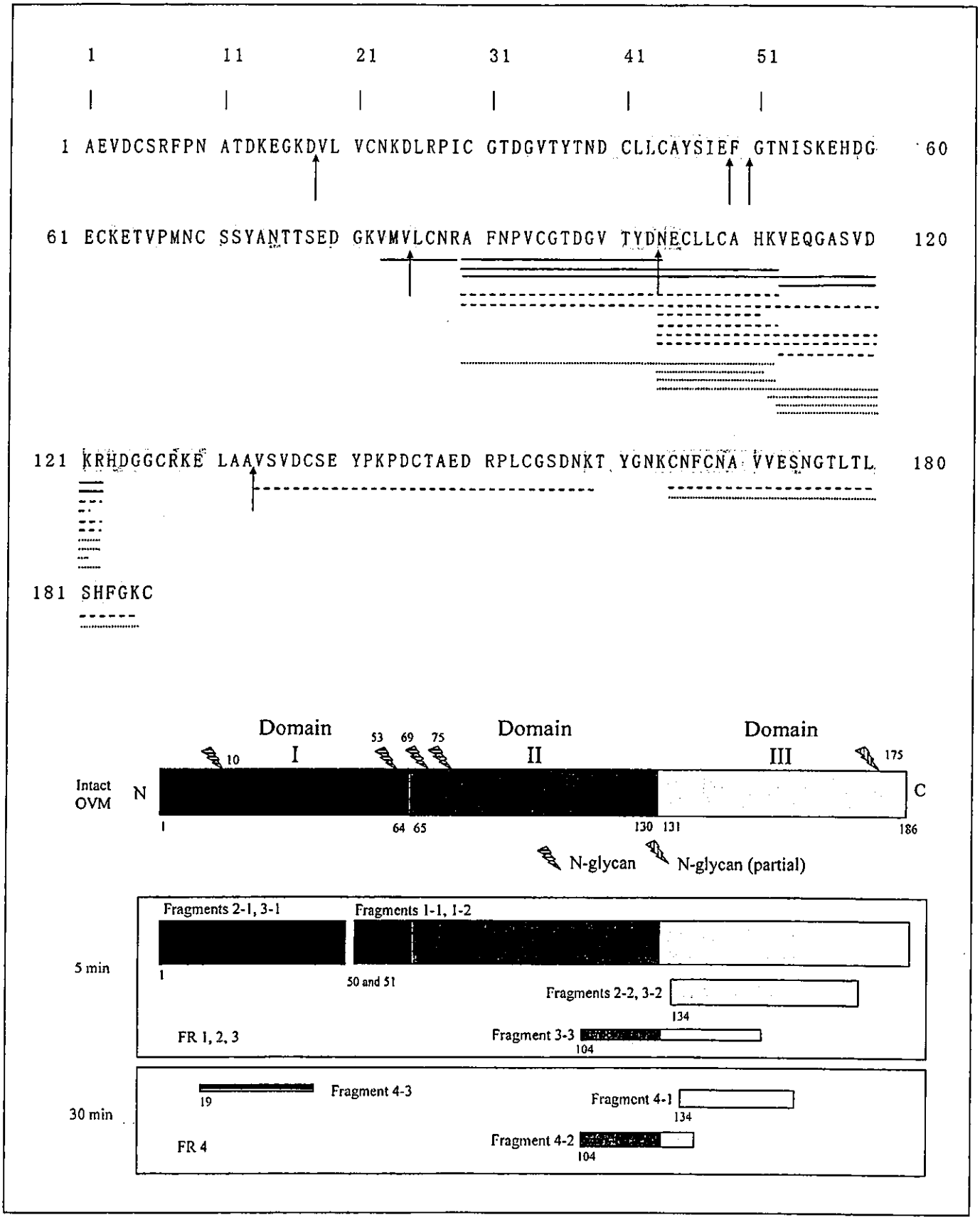
1 11 21 31 41 51
1 AEVDCSRFPN ATDKEGKDVL VCNKDLRPIC GTDGVTYTND CLLCAYSIEF GTNISKEHDG 60
61 ECKETVPMNC SSYANTTSED GKVMVLCNRA FNPVCGTDGV TYDNECLLCA HKVEQGASVD 120
121 KRHDGGCRKE LAAVSVDCSE YPKPDCTAED RPLCGSDNKT YGNKCNFCNA VVESNGTLTL 180
181 SHFGKC
Domain I
Domain II
Domain III
10
53
69
75
175
Intact OVM
N
C
1
64 65
130 131
186
N-glycan
N-glycan (partial)
Fragments 2-1, 3-1
Fragments 1-1, 1-2
5 min
1
50 and 51
Fragments 2-2, 3-2
134
FR 1, 2, 3
Fragment 3-3
104
30 min
19
Fragment 4-3
Fragment 4-1
134
FR 4
Fragment 4-2
104

4

after 5 min of digestion. Three of the serum samples also reacted with FR 2, FR 3, and FR 4 after 30 min of digestion.

The three samples that react with FR 2, FR 3, and FR 4 were obtained from patients who exhibited persistent allergies to egg white. One of these serum samples, No.4, was obtained from a 3-year-old girl who is presently 6 years old; her total IgE level has decreased slightly to 4,450 IU/ml, but the specific IgE level for egg white remains at more than 100 IU/ml, and the patient has not outgrown her hypersensitivity to eggs. Another patient, No. 13, was a 1-year-old boy; 7 years later, his total and egg white-specific IgE levels had been reduced to 947 and 6.85 IU/ml, respectively, but eating raw eggs still caused allergic symptoms. The third FR 4-positive patient, No. 19, was an 11-year-old boy whose total IgE level decreased to 3,940 IU/ml and whose egg white-specific IgE decreased to 13.5 IU/ml after a period of about 2 years; however, this patient has also not outgrown his allergies. These cases and our previously reported data [17] indicate that the induction of egg white tolerance may be difficult in patients whose serum IgE exhibits binding activity to digested small fragments of OVM.

## Discussion

In the SGF-digestion system, preheating the OVM (100°C for 5 or 30 min) did not affect the OVM digestion pattern (fig. 1), consistent with the results of previous reports [9] in which heat treatment did not markedly decrease the allergenicity of OVM. On the other hand, a decrease in the pepsin/OVM ratio dramatically reduced the digestion rate, suggesting that digestibility may vary depending on the amount of OVM intake and the conditions of the individual's digestion system. In its native state, OVM possesses serine protease inhibitor activity. Fu et al. [11] and our group [10] previously reported that intact OVM was stable for 60 min in simulated intestinal fluid. Kovacs-Nolan et al. [15] also reported that pepsin-

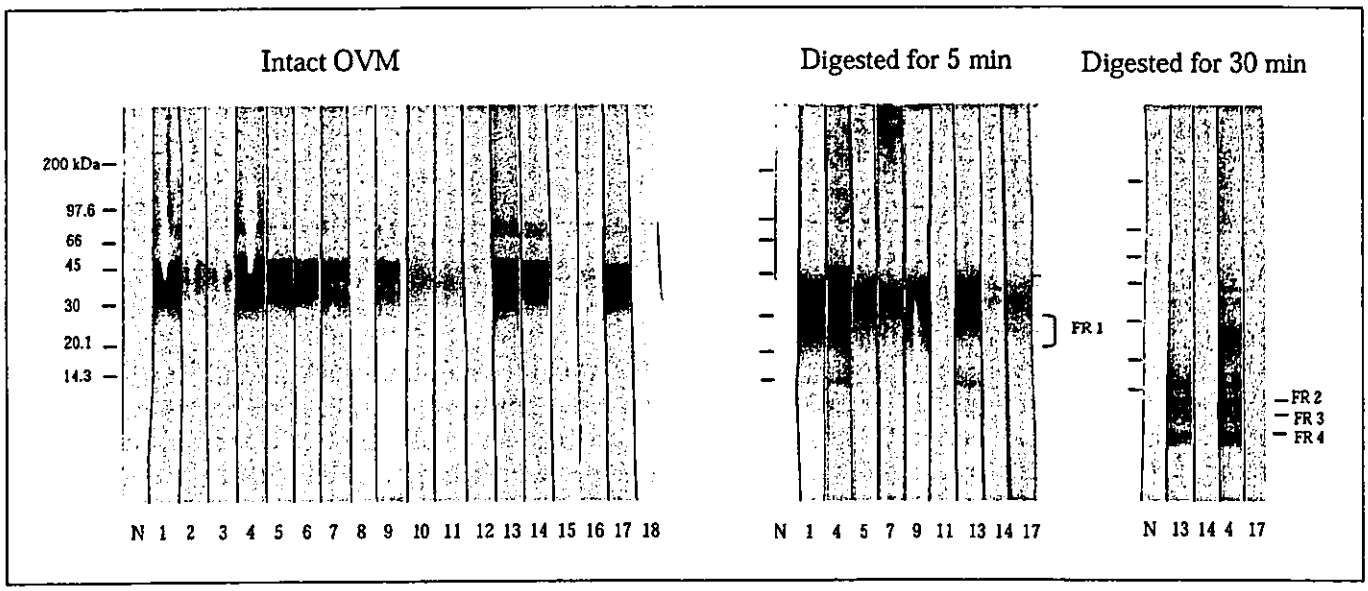


**Fig. 4.** Amino acid sequence and schematic representation of the SGF-digestion pattern of OVM. The amino acid sequence of OVM is shown in the upper panel. The arrows indicate the SGF-digested points according to the results of an N-terminal analysis of the OVM fragments (table 1); and the underlined regions indicate sequences identified by LC/MS/MS. Solid line = FR 1; dotted line = FR 3; dashed line = FR 4. Shaded areas represent reported human IgE epitopes [16]. The lower panel is a summary of the OVM digestion pattern according to N-terminal analysis.

**Fig. 5.** Western blot analysis of intact OVM and the fragments with serum IgE from egg white allergic patients and a normal volunteer. The fragments were prepared as described in the legend of figure 2. The number of each strip corresponds to the sample numbers in table 2.

**Table 3.** Reactivity of OVM and pepsin fragments with patient serum IgE

| No. | IgE content, IU/ml | | Reactivity with patient IgE[1] | | | | |
|---|---|---|---|---|---|---|---|
| | total | egg white-specific | intact OVM | FR 1 | FR 2 | FR 3 | FR 4 |
| 1 | 3,700 | >100 | +++ | ++ | – | – | – |
| 2 | 402 | 3.74 | + | n.d. | n.d. | n.d. | n.d. |
| 3 | 251 | 6.85 | + | n.d. | n.d. | n.d. | n.d. |
| 4 | 6,510 | >100 | +++ | +++ | + | + | ++ |
| 5 | 2,060 | >100 | ++ | ++ | – | – | – |
| 6 | 1,240 | 12.4 | ++ | n.d. | n.d. | n.d. | n.d. |
| 7 | 4,180 | 31.3 | ++ | ++ | – | – | – |
| 8 | 56 | 20.1 | ± | n.d. | n.d. | n.d. | n.d. |
| 9 | 1,355 | 50.7 | ++ | ++ | – | – | – |
| 10 | 22,810 | 2.11 | + | n.d. | n.d. | n.d. | n.d. |
| 11 | 1,463 | 4.65 | + | – | – | – | – |
| 12 | 14,230 | 0.70–3.49 | ± | n.d. | n.d. | n.d. | n.d. |
| 13 | 8,000 | >100 | +++ | +++ | + | + | ++ |
| 14 | 22,490 | 1.05 | +++ | ± | – | – | – |
| 15 | 934 | 66.3 | + | n.d. | n.d. | n.d. | n.d. |
| 16 | 345 | 20.1 | + | n.d. | n.d. | n.d. | n.d. |
| 17 | 1,500 | 80 | ++ | + | – | – | – |
| 18 | 3,300 | >10 | – | n.d. | n.d. | n.d. | n.d. |
| 19 | 20,500 | 26.8 | +++ | ++ | ± | ± | ± |
| 20 | 138 | 45.4 | ++ | + | – | – | – |
| 21 | 940 | 2.44 | + | + | – | – | – |
| 22 | 91 | 0.70–3.49 | + | ± | – | – | – |
| 23 | 828 | 0.9 | ++ | + | – | – | – |
| 24 | 21 | 3.50–17.4 | – | n.d. | n.d. | n.d. | n.d. |
| | positive/tested | | 22/24 (92%)[2] | 13/14 (93%)[3] | 3/14 (21%)[3] | 3/14 (21%)[3] | 3/14 (21%)[3] |

n.d. = Not done.

[1] Intensity of the reactivity of each band was evaluated by the ratio to normal serum: – = <1; ± = 1–2; + = 2–5; ++ = 5–10; +++ = >10.

[2] Percent of egg white-positive samples.

[3] Percent of intact OVM-positive samples.

digested OVM retains its trypsin inhibitor activity. Therefore, OVM and its pepsin-digested fragments were thought to be stable in the small intestine.

At a pepsin/OVM ratio of 1 unit/μg, FR 1 reached a maximum level after 2 min of digestion, while both FR 2 and FR 3 reached maximum levels after 5 min of digestion; thereafter, FR 1, FR 2, and FR 3 gradually decreased. However, FR 4 increased continuously throughout the 30-min period of digestion and the major fragments were seen after 30 min of digestion (fig. 3). FR 4 was mainly composed of three fragments whose N-terminals were 134V, 104N and 19V (table 1). A C-terminal sequence, 165N–185C, was also identified in FR 4 (table 2). These fragments contain known IgE epitopes [19] and therefore may cause allergic responses. Three of the OVM-positive sera from patients with egg white allergy reacted positively with the FR 4 fragments (table 3).

The present results are consistent with the previous finding that pediatric subjects with a higher IgE-binding activity to pepsin-treated OVM were unlikely to outgrow their egg allergy [17]. For peanut allergies, differences in IgE-binding epitopes have been reported between the patients with clinically active peanut allergies and those who developed a tolerance, regardless of the presence of high or low peanut-specific IgE levels [20].

The N-terminal residue of the major fragment (4-1) of FR 4 was Val-134 (30%; table 1). This fragment retains most of domain III, which has been reported to have significantly higher human IgG- and IgE-binding activities than those of domains I and II [12]. A domain-III OVM

variant has also been reported to cause a reduction in immunogenicity and allergenicity [21].

Domains I, II, and III contain one, three, and one N-glycosylation sites, respectively [7]. The possible relation between the carbohydrate chain in domain III and allergenicity is interesting. One report suggested that this carbohydrate chain may play an important role in allergenic determinants against human IgE antibody [13], and another report suggested that the carbohydrate chains of OVM may protect against peptic hydrolysis [22]. However, the carbohydrate moieties have been shown to have only a minor effect on allergenicity [23]. As shown in figure 2, intact OVM, FR 1, and FR 2 fragments were detected using PAS staining, suggesting the presence of carbohydrate chains, but FR 4 was not stained with the PAS reagent, despite being clearly detected with CBB. Therefore, FR 4 might contain little or no carbohydrate chains. Since FR 4 seems to maintain its allergenic potential, as described above, the absence of the carbohydrate chains in FR 4 suggests that they are not necessary for OVM allergenicity. Since the minimum peptide size capable of eliciting significant clinical symptoms of allergic reactions is thought to be 3.1 kDa [24], FR 4 may be able to trigger mast cell activation and elicit clinical symptoms.

In this report, the SGF-digestion kinetic pattern of OVM was investigated in detail, and the partial sequences of the fragments in the 4 fractions separated by SDS-PAGE were determined. Furthermore, the reactivity of the fragments with a number of serum samples from patients with egg white allergies was detected using Western blotting. The four fractions were separated according to their molecular weight and consisted of more than one fragment, as determined by N-terminal analysis. The identified sequences that started at Asn-104 and Val-134 in FR 3, as determined using LC/MS/MS (table 2), coincided with the 3-2 and 3-3 fragments in the N-terminal analysis (table 1), and the sequence that started at Asn-104 in FR 4 coincided with fragment 4-2. Moreover, the LC/MS/MS analysis indicated that FR 3 and FR 4 contained other parts of domain II and the C-terminal sequence N165–C185, which are thought to be minor components of these fractions. The combination of SGF digestion and patient IgE may provide useful information for the diagnosis and prediction of potential OVM allergenicity.

## Acknowledgement

This study was supported by a grant from the Ministry of Health, Labor and Welfare, and the Cooperative System for Supporting Priority Research of Japan Science and Technology Agency.

## References

1 Sampson HA, McCaskill CC: Food hypersensitivity and atopic dermatitis: Evaluation of 113 patients. J Pediatr 1985;107:669–675.
2 Bock SA, Sampson HA, Atkins FM, Zeiger RS, Lehrer S, Sachs M, Bush RK, Metcalfe DD: Double-blind, placebo-controlled food challenge (DBPCFC) as an office procedure: A manual. J Allergy Clin Immunol 1988;82:986–997.
3 Bock SA, Atkins FM: Patterns of food hypersensitivity during sixteen years of double-blind, placebo-controlled food challenges. J Pediatr 1990;117:561–567.
4 Boyano-Martinez T, Garcia-Ara C, Diaz-Pena JM, Martin-Esteban M: Prediction of tolerance on the basis of quantification of egg white-specific IgE antibodies in children with egg allergy. J Allergy Clin Immunol 2002;110:304–309.
5 Kotaniemi-Syrjanen A, Reijonen TM, Romppanen J, Korhonen K, Savolainen K, Korppi M: Allergen-specific immunoglobulin E antibodies in wheezing infants: The risk for asthma in later childhood. Pediatrics 2003;111:e255–e261.
6 Li-Chan E, Nakai S: Biochemical basis for the properties of egg white. Crit Rev Poultry Biol 1989;2:21–58.
7 Kato I, Schrode J, William J. Kohr WJ, Laskowski M Jr: Chicken ovomucoid: Determination of its amino acid sequence, determination of the trypsin reactive site, and preparation of all three of its domains. Biochemistry 1987;26:193–201.
8 Matsuda T, Watanabe K, Nakamura R: Immunochemical and physical properties of peptic-digested ovomucoid. J Agric Food Chem 1983;31:942–946.
9 Honma K, Aoyagi M, Saito K, Nishimuta T, Sugimoto K, Tsunoo H, Niimi H, Kohno Y: Antigenic determinants on ovalbumin and ovomucoid: Comparison of the specificity of IgG and IgE antibodies. Arerugi 1991;40:1167–1175.
10 Takagi K, Teshima R, Okunuki H, Sawada J: Comparative study of in vitro digestibility of food proteins and effect of preheating on the digestion. Biol Pharm Bull 2003;26:969–973.
11 Fu TJ, Abbott UR, Hatzos C: Digestibility of food allergens and nonallergenic proteins in simulated gastric fluid and simulated intestinal fluid-a comparative study. J Agric Food Chem 2002;50:7154–7160.
12 Zhang JW, Mine Y: Characterization of IgE and IgG epitopes on ovomucoid using egg-white-allergic patients' sera. Biochem Biophys Res Commun 1998;253:124–127.
13 Matsuda T, Nakamura R, Nakashima I, Hasegawa Y, Shimokata K: Human IgE antibody to the carbohydrate-containing third domain of chicken ovomucoid. Biochem Biophys Res Commun 1985;129:505–510.
14 Thomas K, Aalbers M, Bannon GA, Bartels M, Dearman RJ, Esdaile DJ, Fu TJ, Glatt CM, Hadfield N, Hatzos C, Hefle SL, Heylings JR, Goodman RE, Henry B, Herouet C, Holsapple M, Ladics GS, Landry TD, MacIntosh SC, Rice EA, Privalle LS, Steiner HY, Teshima R, Van Ree R, Woolhiser M, Zawodny J: A multilaboratory evaluation of a common in vitro pepsin digestion assay protocol used in assessing the safety of novel proteins. Regul Toxicol Pharmacol 2004;39:87–98.

15 Kovacs-Nolan J, Zhang JW, Hayakawa S, Mine Y: Immunochemical and structural analysis of pepsin-digested egg white ovomucoid. J Agric Food Chem 2000;48:6261–6266.
16 Besler M, Petersen A, Steinhart H, Paschke A: Identification of IgE-Binding Peptides Derived from Chemical and Enzymatic Cleavage of Ovomucoid (Gal d 1). Internet Symposium on Food Allergens 1999;1:1–12. http://www.food-allergens.de
17 Urisu A, Yamada K, Tokuda R, Ando H, Wada E, Kondo Y, Morita Y: Clinical significance of IgE-binding activity to enzymatic digests of ovomucoid in the diagnosis and the prediction of the outgrowing of egg white hypersensitivity. Int Arch Allergy Immunol 1999; 120:192–198.
18 Zacharius RM, Zell TE, Morrison JH, Woodlock JJ: Glycoprotein staining following electrophoresis on acrylamide gels. Anal Biochem 1969;30:148–152.
19 Mine Y, Zhang JW: Identification and fine mapping of IgG and IgE epitopes in ovomucoid. Biochem Biophys Res Commun 2002; 292:1070–1074.
20 Beyer K, Ellman-Grunther L, Jarvinen KM, Wood RA, Hourihane J, Sampson HA: Measurement of peptide-specific IgE as an additional tool in identifying patients with clinical reactivity to peanuts. J Allergy Clin Immunol 2003;112:202–207.
21 Mine Y, Sasaki E, Zhang JW: Reduction of antigenicity and allergenicity of genetically modified egg white allergen, ovomucoid third domain. Biochem Biophys Res Commun 2003; 302:133–137.
22 Matsuda T, Gu J, Tsuruta K, Nakamura R: Immunoreactive glycopeptides separated from peptic hydrolysate of chicken egg white ovomucoid. J Food Sci 1985;50:592–594.
23 Cooke SK, Sampson HA: Allergenic properties of ovomucoid in man. J Immunol 1997;159: 2026–2032.
24 Kane PM, Holowka D, Baird B: Cross-linking of IgE receptor complexes by rigid bivalent antigens greater than 200 Å in length triggers cellular degranulation. J Cell Biol 1988;107: 969–980.

〔シンポジウム：プロテオミクスの新技術―電気泳動とマススペクトロメトリー―〕

# LC/MS/MSを用いた糖タンパク質の糖鎖解析 ―糖鎖結合位置及び結合糖鎖の解析―

伊藤さつき・原園　景・川崎ナナ・橋井則貴・松石　紫・川西　徹・早川堯夫


## SUMMARY

Liquid chromatography/tandem mass spectrometry (LC/MS/MS) is a powerful tool for the analysis of glycosylation sites and of site-specific glycosylation in a glycoprotein. The glycopeptides in a complex mixture of tryptic digest can be separated and monitored by using oxonium ions produced from a carbohydrate moiety through CID-MS/MS. Based on b and y ions in the product ion mass spectra, peptides can be identified, and the structure of carbohydrates can be deduced from B ions and the molecular weight of precursor glycopeptide. Here we show the site-specific glycosylation analysis of α-fetoprotein and an SDS-PAGE gel-separated GPI-anchored protein.


Key words: LC/MS/MS, glycopeptide, product ion scan, QqTOF-MS, gel-separated protein.

## はじめに

生体内に存在する全タンパク質の半分以上が糖鎖付加を受けていると言われるように，糖鎖付加は，主要な翻訳後修飾の1つである．糖タンパク質の糖鎖部分には，結合部位ごとに不均一性が存在し，病気・発生・老化等によって変化することが知られている[1～3]．様々な生命現象における糖タンパク質の糖鎖の役割を解明するためには，結合する糖鎖構造の変化を明らかにすることはもちろんであるが，構造が変化した糖鎖がどの位置に結合していたかを明らかにすることが重要である．

液体クロマトグラフィー／タンデム質量分析法（LC/MS/MS）は，タンパク質の酵素消化によって得られたペプチドと糖ペプチドの混合物をLCで分離しながら，オンラインでMS/MS分析を行うのに用いられている．糖ペプチドのプロダクトイオンスペクトルにはペプチドだけでなく，糖鎖構造に関する多くの情報が含まれているので，LC/MS/MSは部位特異的糖鎖解析に非常に有用である．しかし，無数のペプチドピークの中から糖ペプチドピークを特定するのは難しく，いかに糖ペプチドのピークを選別するかが，糖ペプチド解析の鍵となっている．

ペプチド・糖ペプチドの中から，糖ペプチドを選別する方法として，LC上で選別する方法と，MS/MSで選別する方法がある．前者の方法として，$C_{18}$カラムと酢酸アンモニウム系溶離液を用いて糖ペプチドだけを選択的に溶出させる方法[4]や，レクチンカラムを用いて糖ペプチドを回収し，さらにHPLCで分離するグライコキャッチ法[5]等が報告されている．MS/MSで選別する方法としては，糖鎖に特徴的なオキソニウムイオン（$[HexNAc]^+$; $m/z$ 204, $[Hex\text{-}HexNAc]^+$; $m/z$ 366等）を利用して，糖ペプチドを特定する方法が知られ，インソースフラグメンテーション[6]や，プリカーサーイオンスキャン[7,8]を利用した方法が報告されている．インソースフラグメンテーションを用いた場合，クロマトグラム上でのおおよその糖ペプチドの溶出位置を特定することはできるが，プリカーサーイオンを特定することができず，溶出位置付近のマススペクトル及びプロダクトイオンスペクトルの特徴から，糖ペプチドのイオンを特定しなければならない．これに対して，プリカーサーイオンスキャンは，糖ペプチドイオンを特定することはできるが，プロダクトイオンスペクトルが得られないため，ペプチドや糖鎖に関する情報が得られないといった問題がある．

そこで，我々は，得られた無数のペプチド・糖ペプチドのプロダクトイオンスペクトルの中から，オキソニウムイオンを指標として，糖ペプチドに由来するプロダクトイオ

---

Glycosylation analysis of glycoproteins by LC/MS/MS: analysis of glycosylation sites and of site-specific heterogeneity.

Satsuki Itoh, Akira Harazono, Nana Kawasaki, Noritaka Hashii, Yukari Matsuishi, Toru Kawanishi, Takao Hayakawa; 国立医薬品食品衛生研究所

Correspondence address: Nana Kawasaki; National Institute of Health Science, 1-18-1, Kamiyoga, Setagaya-ku, Tokyo 158-8501, Japan.

第54回日本電気泳動学会シンポジウム

（受付2004年10月4日，受理2004年10月28日，刊行2004年12月15日）

ンスペクトルを選択的に取り出し，ペプチドを同定すると同時に，結合糖鎖を解析する方法を用いている[9,10]．以下に四重極飛行時間型質量分析計（quadrupole time of flight-MS, QqTOF-MS）を用いて，部位特異的に糖タンパク質の糖鎖を解析した例として，α-フェトプロテイン（AFP）と，電気泳動で分離されたラット脳内 Glycosylphosphatidylinositol（GPI）アンカー型タンパク質の分析を紹介する．

## I. LC/MS/MS を用いた糖タンパク質の糖鎖構造解析 —α-フェトプロテイン（AFP）の解析—

血液中に存在する糖タンパク質の中には，疾患等により結合糖鎖構造が変化することから，診断マーカーとして用いられているものがあり[11]，その代表的なタンパク質として AFP が知られている．AFP は，N-結合型糖鎖付加部位（Asn233）が一箇所存在する分子量約 68,000 の血清糖タンパク質で，肝細胞癌において，還元末端 GlcNAc のフコシル化率が増加することから，レクチンアフィニティー電気泳動とイムノブロットを用いた早期診断に利用されている[12,13]．LC/MS/MS を用いて，AFP の糖鎖を詳細に解析できるようになれば，今後，より簡便に，且つ微量のサンプルで，早期診断が可能になることが期待される．ここでは，臍帯血由来 AFP について解析を行った例を示す．

Fig. 1（A）は，AFP を還元カルボキシメチル化し，脱塩後，トリプシン消化を行い，LC/MS 分析を行ったものである．ペプチド・糖ペプチド混合物のため多くのイオンが検出されているが，データ依存的 MS/MS データ（Fig. 1（B））の中の *m/z* 204（$[HexNAc]^+$）をモニターすることによって（Fig. 1（C）），糖ペプチドに由来するプロダクトイオンスペクトルを取り出すことができる．

例えば，Fig. 2 は，24 分に溶出された糖ペプチド（*m/z* $1061.8^{+3}$）のプロダクトイオンスペクトルである．低分子量側に，*m/z* 204（$[HexNAc]^+$）に加えて，糖鎖に由来する *m/z* 168（$[HexNAc\text{-}2H_2O]^+$），*m/z* 186（$[HexNAc\text{-}H_2O]^+$）及び *m/z* 366（$[Hex\text{-}HexNAc]^+$）や，シアロ糖鎖に由来する *m/z* 292（$[NeuAc]^+$）及び *m/z* 274（$[NeuAc\text{-}H_2O]^+$）の B イオンが検出されている．高分子量側には，ペプチド VNFTEIQK に由来するイオン（*m/z* 978.5）と，b 及び y イオンが検出されている．Fig. 2 中の表はペプチド VNFTEIQK から生じる b 及び y イオンの理論 *m/z* 値を示し，その中で太字で示された値は，実際，プロダクトイオンスペクトル上で検出されたイオンを示している．さらに，ペプチドに HexNAc が 1 または 2 分子，さらに Hex が 1～3 分子結合したイオンが検出され，N-結合型糖鎖のコア部分を確認することができる．糖鎖構造は，プロダクトイオンスペクトル上の B イオンと，TOF-MS で得られた糖ペプチドの分子量（3182.3 Da）からペプチドの理論分子量（977.5 Da）を差し引くことにより得られた分子量（2222.8 Da）から，シアル酸が 2 分子結合した 2 本鎖糖鎖であると推定される．このように，*m/z* 204 が検出されたプロダクトイオンスペクトルとそのプリカーサーイオンを解析することによって，AFP に結合する糖鎖を推定することが可能である（Table 1）．

臍帯血由来 AFP の結合糖鎖は，これまでにメチル化分析やレクチン分画等によって分析されており，主にジシアロ 2 本鎖型糖鎖であることが報告されている[14]．今回の LC/MS/MS 分析の結果で，その他に，アシアロ糖鎖，3 本鎖糖鎖や混成型糖鎖等が結合していることが示唆され，簡単な操作で，より詳細に糖鎖構造が解析できることがわかる．

以上のように，オキソニウムイオンを指標として，糖ペプチドのプロダクトイオンスペクトルを選び出す方法は，ペプチドの b, y イオン及び糖鎖の B イオンをもとにペプチドの同定と結合糖鎖の構造推定を行うことが可能であることから，部位特異的糖鎖構造解析に有用である．次に，LC/MS/MS による糖ペプチド解析法を，電気泳動法で分離された糖タンパク質の解析に応用した例を示す．

## II. ゲル内糖タンパク質の糖鎖構造解析 —ラット脳内 GPI アンカー型タンパク質の解析—

脳・神経系の細胞膜上には，細胞間認識やシグナル伝達に関与する多数の糖タンパク質が存在し，糖鎖はこれらの

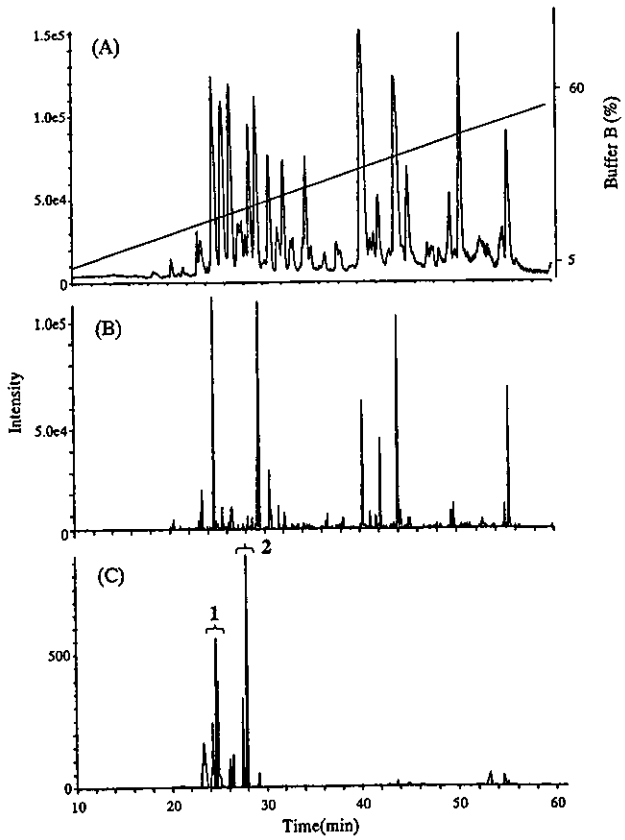


Fig. 1. LC/MS/MS of AFP, (A) TOF-MS full scan at *m/z* 700–2000, (B) product ion scan at *m/z* 100-2000, (C) product ion scan at *m/z* 204.

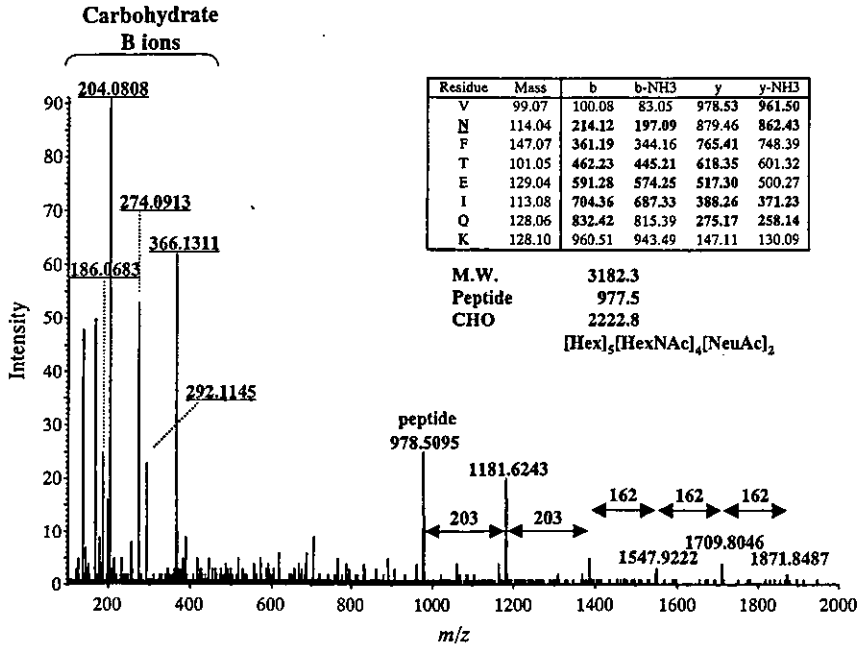


Fig. 2. Product ion spectrum of a glycopeptide (*m/z* 1061.83$^{3+}$) at 24 min.

Inset table shows theoretical *m/z* values of b and y ions, and ions detected by MS/MS are indicated by bold face.

Table 1. Glycosylation analysis of AFP

| Peak No. | Peptide sequence (theoretical peptide mass[a]) | Retention time (min) | Observed *m/z* (charge) | Carbohydrate composition | Calculated Carbohydrate mass | Theoretical carbohydrate mass[a] |
|---|---|---|---|---|---|---|
| 1 | KVNFTEIQKL (977.5) | 23 | 1013.43(3) | $[dHex]_1[Hex]_5[HexNAc]_4[NeuAc]_1$ | 2077.8 | 2077.7 |
| | | 23 | 1519.67(2) | $[dHex]_1[Hex]_5[HexNAc]_4[NeuAc]_1$ | 2077.8 | 2077.7 |
| | | 23 | 1081.29(3) | $[dHex]_1[Hex]_5[HexNAc]_5[NeuAc]_1$ | 2281.4 | 2280.8 |
| | | 23 | 1621.44(2) | $[dHex]_1[Hex]_5[HexNAc]_5[NeuAc]_1$ | 2281.4 | 2280.8 |
| | | 23 | 1446.62(2) | $[Hex]_5[HexNAc]_4[NeuAc]_1$ | 1931.8 | 1931.7 |
| | | 23 | 1118.67(2) | $[Hex]_4[HexNAc]_3$ | 1275.9 | 1275.5 |
| | | 23 | 1264.05(2) | $[Hex]_4[HexNAc]_3[NeuAc]_1$ | 1566.6 | 1566.6 |
| | | 23 | 1110.48(3) | $[Hex]_4[HexNAc]_3[NeuAc]_1$ | 1566.6 | 1566.6 |
| | | 24 | 1665.44(2) | $[dHex]_1[Hex]_5[HexNAc]_4[NeuAc]_2$ | 2369.4 | 2368.8 |
| | | 24 | 1178.33(3) | $[dHex]_1[Hex]_5[HexNAc]_5[NeuAc]_2$ | 2572.5 | 2571.9 |
| | | 24 | 1061.78(3) | $[Hex]_5[HexNAc]_4[NeuAc]_2$ | 2222.9 | 2222.8 |
| | | 25 | 1592.17(2) | $[Hex]_5[HexNAc]_4[NeuAc]_2$ | 2222.9 | 2222.8 |
| 2 | KFTKVNFTEIQKL (1353.7) | 27 | 1236.04(3) | $[dHex]_1[Hex]_5[HexNAc]_4[NeuAc]_2$ | 2369.4 | 2368.8 |
| | | 27 | 1853.29(2) | $[dHex]_1[Hex]_5[HexNAc]_4[NeuAc]_2$ | 2369.4 | 2368.8 |
| | | 27 | 1187.17(3) | $[Hex]_5[HexNAc]_4[NeuAc]_2$ | 2222.8 | 2222.8 |
| | | 28 | 1780.23(2) | $[Hex]_5[HexNAc]_4[NeuAc]_2$ | 2222.8 | 2222.8 |
| | | 28 | 1303.56(3) | $[dHex]_1[Hex]_5[HexNAc]_5[NeuAc]_2$ | 2572.0 | 2571.9 |
| | | 28 | 1138.84(3) | $[dHex]_1[Hex]_5[HexNAc]_4[NeuAc]_1$ | 2077.8 | 2077.7 |
| | | 28 | 1206.52(3) | $[dHex]_1[Hex]_5[HexNAc]_5[NeuAc]_1$ | 2280.9 | 2280.8 |
| | | 28 | 1090.14(3) | $[Hex]_5[HexNAc]_4[NeuAc]_1$ | 1931.7 | 1931.7 |
| | | 28 | 1322.75(3) | $[Hex]_5[HexNAc]_6[NeuAc]_2$ | 2629.6 | 2628.9 |

[a] Monoisotopic mass value.

機能に深く関わっていると考えられている[15]．しかし，微量膜タンパク質であることから，精製が困難で，解析に必要な量が得られず，多くの糖タンパク質の糖鎖構造は明らかにされていない．タンパク質混合物の分離に適した電気泳動と LC/MS/MS を活用することによって，これらの糖鎖構造を解析できると期待される．以下は，GPI を介して膜に結合する GPI アンカー型タンパク質の糖鎖解析を行った例である．

ラット脳の膜画分から，Phosphatidylinositol-specific phospholipase C (PIPLC) 消化によって得られた可溶性 GPI アンカー型タンパク質群を，還元カルボキシアミドメチル化後，SDS-PAGE で分離した (Fig. 3)．通常，ゲル内のタ

ンパク質同定は，ゲル内プロテアーゼ消化後，抽出されたペプチドのみを用いて行われているが，糖鎖構造解析を行う場合，すべての糖ペプチド断片を同程度の収率で回収する必要がある．そこで，ゲルより糖タンパク質を抽出後，トリプシン消化を行う方法を選んだ．

Fig. 4 (A) は，バンド1を切り出し，1%SDS を用いてタンパク質を抽出後，トリプシン消化を行い，LC/MS/MS 分析を行ったものである．まず，データベース検索の結果，バンド1は，Thy-1 と同定された．Thy-1 は，免疫グロブリンスーパーファミリーに属する GPI アンカー型タンパク質であり，3 箇所の N-結合型糖鎖付加部位 (Asn23, 74, 98) を有するアミノ酸残基数 111 の糖タンパク質である (Fig. 5)．

次に，AFP と同様に，*m/z* 204 を指標として，全ペプチドのプロダクトイオンスペクトルの中から，糖ペプチドのプロダクトイオンスペクトルを選択的に取り出した (Fig. 4 (C))．それらのプロダクトイオンスペクトル及びプリカーサーイオンの TOF-MS から，T1 及び T2 に溶出された糖ペプチドは，それぞれ高マンノース型糖鎖が結合した Asn23 を含む糖ペプチド，His21-Phe33，及び His21-Arg37 であり，T3 及び T4 は，複合型及び混成型糖鎖が結合した Asn74 を含む糖ペプチド，Val69-Lys78 であることが判った (Table 2)．

Fig. 6 は，T3 に溶出された糖ペプチドのうち，*m/z* $1532.2^{+2}$ を示す糖ペプチドのプロダクトイオンスペクトルである．低分子量側に，AFP で検出されたイオン，*m/z* 168, 186, 204, 366 に加え，*m/z* 528 ($[Hex]_2[HexNAc]^+$)，*m/z* 569 ($[Hex][HexNAc]_2^+$) や，*m/z* 512 ($[Hex][HexNAc][dHex]^+$) 等の B イオンが検出されており，Gal1-3(4)(Fuc1-4(3))-GlcNAc 構造を含むことが推定される．高分子量側には，ペプチドに由来するイオン (*m/z* 1107.6) と b 及び y イオンが検出され，VLTLANFTTK と同定された (Fig. 6 中の表)．また，ペプチドに HexNAc，HexNAc-HexNAc，HexNAc-HexNAc-Hex が結合したイオンが検出されている他，さらに，これらに dHex が1分子結合したイオンが検出されていることから，結合糖鎖のコア部分がフコシル化されていることが判る．結合糖鎖は，TOF-MS で得られた糖ペプチドの分子量 (3062.4 Da) から，ペプチドの理論分子量 (1106.6 Da) を差し引くことにより得られた糖鎖分子量 (1973.7 Da) から，Fig. 6 中に示すような構造であると推定される．Table 2 は，同様に解析した結果，Thy-1 に結合すると推定された糖鎖構造である．

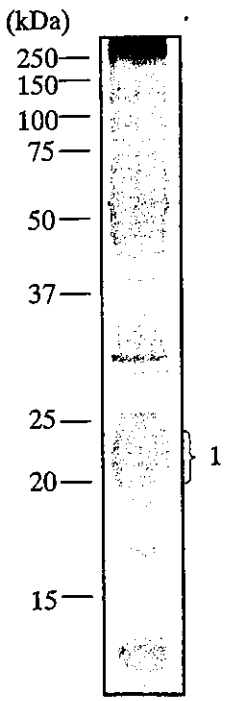


Fig. 3. SDS-PAGE of lipid-free GPI-anchored protein prepared from rat brain.

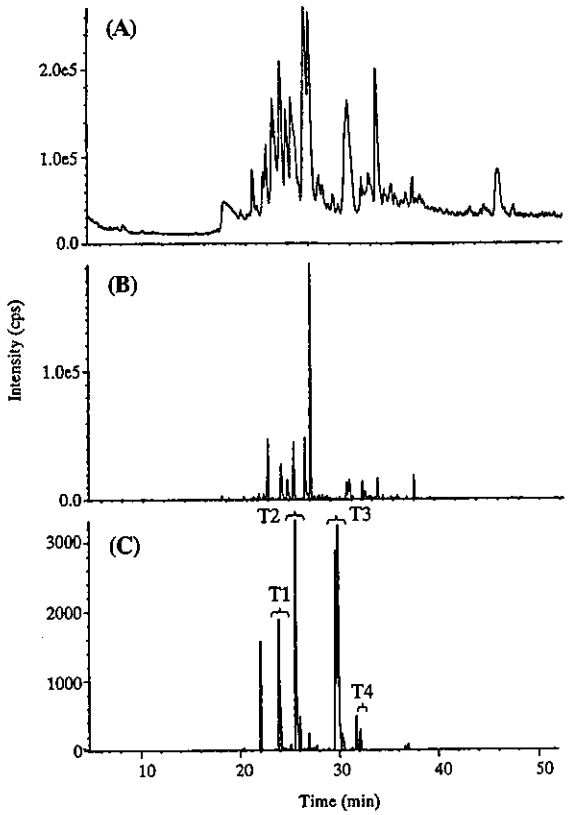


Fig. 4. LC/MS/MS of rat brain Thy-1, (A) TOF-MS full scan at *m/z* 700–2000, (B) product ion scan at *m/z* 100–2000, (C) Product ion scan at *m/z* 204.

QRVISLTACL VNQNLRLDCR HENNTNLPIQ HEFSLTREKK KHVLSGTLGV
50
PEHTYRSRVN LFSDRFIKVL TLANFTTKDE GDYMCELRVS GQNPTSSNKT
100
INVIRDKLVK C
GPI-anchor

Fig. 5. Amino acid sequence of rat Thy-1.

Glycopeptides produced by trypsin are underlined. N-glycosylation sites are indicated by bold face.

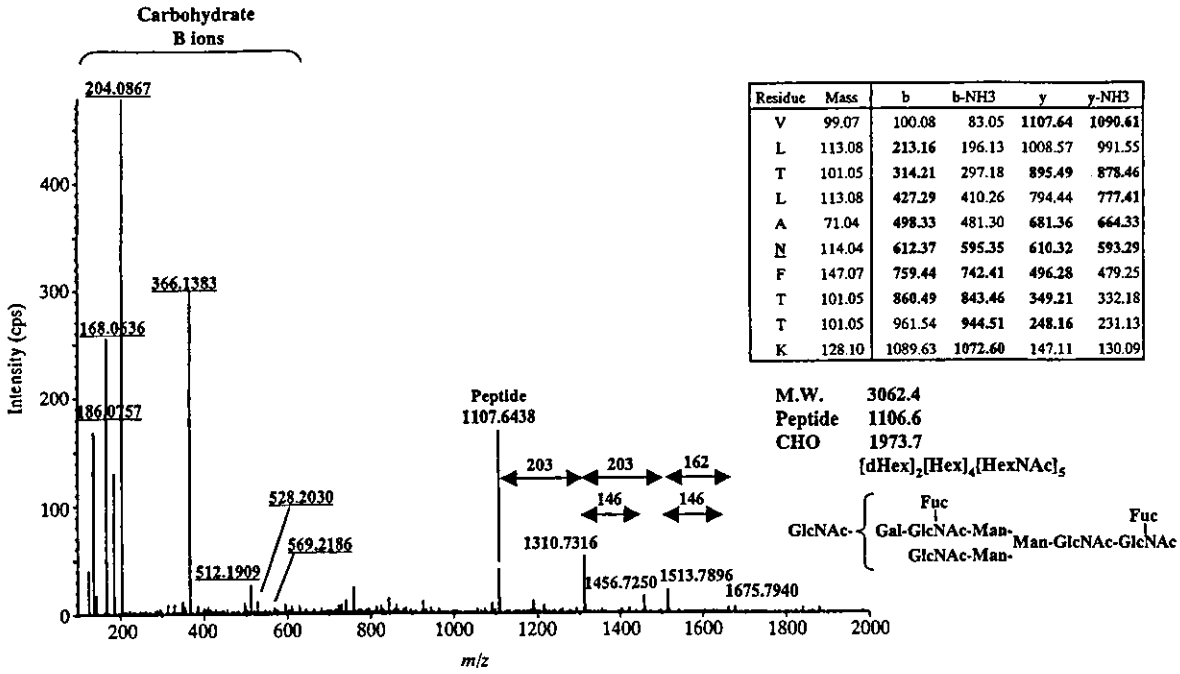


| Residue | Mass | b | b-NH3 | y | y-NH3 |
|---|---|---|---|---|---|
| V | 99.07 | 100.08 | 83.05 | 1107.64 | 1090.61 |
| L | 113.08 | 213.16 | 196.13 | 1008.57 | 991.55 |
| T | 101.05 | 314.21 | 297.18 | 895.49 | 878.46 |
| L | 113.08 | 427.29 | 410.26 | 794.44 | 777.41 |
| A | 71.04 | 498.33 | 481.30 | 681.36 | 664.33 |
| N | 114.04 | 612.37 | 595.35 | 610.32 | 593.29 |
| F | 147.07 | 759.44 | 742.41 | 496.28 | 479.25 |
| T | 101.05 | 860.49 | 843.46 | 349.21 | 332.18 |
| T | 101.05 | 961.54 | 944.51 | 248.16 | 231.13 |
| K | 128.10 | 1089.63 | 1072.60 | 147.11 | 130.09 |

Fig. 6. Product ion spectrum of a glycopeptide (*m/z* 1532.2$^{2+}$) at peak 29.5 min. Inset table shows theoretical *m/z* values of b and y ions, and ions detected by MS/MS are indicated by bold face.

Table 2. Glycosylation analysis of rat brainThy-1

| Peak No. | Peptide sequence (theoretical peptide mass[a]) | Glycosylation site | Retention time (min) | Observed *m/z* (charge) | Carbohydrate composition | Calculated carbohydrate mass | Theoretical carbohydrate mass[a] |
|---|---|---|---|---|---|---|---|
| T1 | H21-F33 (1591.73) | N23 | 23.9 | 991.1(3) | $[Hex]_6[HexNAc]_2$ | 1396.6 | 1396.5 |
| | | | 23.9 | 1486.2(2) | $[Hex]_6[HexNAc]_2$ | 1396.6 | 1396.5 |
| | | | 23.9 | 1045.1(3) | $[Hex]_7[HexNAc]_2$ | 1558.7 | 1558.5 |
| | | | 24.0 | 1567.2(2) | $[Hex]_7[HexNAc]_2$ | 1558.6 | 1558.5 |
| | | | 24.0 | 937.1(3) | $[Hex]_5[HexNAc]_2$ | 1234.5 | 1234.4 |
| | | | 24.0 | 1405.1(2) | $[Hex]_5[HexNAc]_2$ | 1234.5 | 1234.4 |
| T2 | H21-R37 (2048.99) | N23 | 25.5 | 1197.6(3) | $[Hex]_7[HexNAc]_2$ | 1558.6 | 1558.5 |
| | | | 25.6 | 1143.5(3) | $[Hex]_6[HexNAc]_2$ | 1396.6 | 1396.5 |
| | | | 25.6 | 857.9(4) | $[Hex]_6[HexNAc]_2$ | 1396.6 | 1396.5 |
| | | | 25.7 | 1089.5(3) | $[Hex]_5[HexNAc]_2$ | 1234.5 | 1234.4 |
| | | | 25.7 | 817.4(4) | $[Hex]_5[HexNAc]_2$ | 1234.6 | 1234.4 |
| | | | 25.9 | 1633.8(2) | $[Hex]_5[HexNAc]_2$ | 1234.5 | 1234.4 |
| T3 | V69-K78 (1106.62) | N74 | 29.5 | 1686.3(2) | $[dHex]_3[Hex]_5[HexNAc]_5$ | 2282.0 | 2281.9 |
| | | | 29.6 | 1124.5(3) | $[dHex]_3[Hex]_5[HexNAc]_5$ | 2282.0 | 2281.9 |
| | | | 29.6 | 1532.2(2) | $[dHex]_2[Hex]_4[HexNAc]_5$ | 1973.9 | 1973.7 |
| | | | 29.6 | 1021.8(3) | $[dHex]_2[Hex]_4[HexNAc]_5$ | 1973.9 | 1973.7 |
| | | | 29.7 | 1162.6(2) | $[Hex]_5[HexNAc]_2$ | 1234.5 | 1234.4 |
| | | | 29.7 | 1491.2(2) | $[dHex]_2[Hex]_6[HexNAc]_3$ | 1891.8 | 1891.7 |
| | | | 29.7 | 1592.8(2) | $[dHex]_2[Hex]_6[HexNAc]_4$ | 2094.9 | 2094.8 |
| | | | 29.8 | 1378.2(2) | $[dHex]_1[Hex]_3[HexNAc]_5$ | 1665.7 | 1665.6 |
| | | | 29.9 | 919.1(3) | $[dHex]_1[Hex]_3[HexNAc]_5$ | 1665.7 | 1665.6 |
| | | | 29.8 | 1438.7(2) | $[dHex]_1[Hex]_5[HexNAc]_4$ | 1786.8 | 1786.7 |
| | | | 30.3 | 959.5(3) | $[dHex]_1[Hex]_5[HexNAc]_4$ | 1786.8 | 1786.7 |
| | | | 29.9 | 1511.7(2) | $[dHex]_2[Hex]_5[HexNAc]_4$ | 1932.8 | 1932.7 |
| | | | 30.0 | 1008.1(3) | $[dHex]_2[Hex]_5[HexNAc]_4$ | 1932.8 | 1932.7 |
| | | | 30.0 | 1519.7(2) | $[dHex]_1[Hex]_6[HexNAc]_4$ | 1948.8 | 1948.7 |
| | | | 30.0 | 1572.2(2) | $[dHex]_2[Hex]_7[HexNAc]_3$ | 2053.9 | 2053.7 |
| | | | 30.1 | 1499.2(2) | $[dHex]_1[Hex]_7[HexNAc]_3$ | 1907.8 | 1907.7 |
| | | | 30.2 | 1276.6(2) | $[dHex]_1[Hex]_3[HexNAc]_4$ | 1462.6 | 1462.5 |
| | | | 30.2 | 1337.2(2) | $[dHex]_1[Hex]_5[HexNAc]_3$ | 1583.7 | 1583.6 |
| | | | 31.7 | 1860.4(2) | $[dHex]_2[Hex]_5[HexNAc]_6[NeuAc]_1$ | 2630.1 | 2630.0 |
| | | | 31.7 | 1240.6(3) | $[dHex]_2[Hex]_5[HexNAc]_6[NeuAc]_1$ | 2630.1 | 2630.0 |
| | | | 31.9 | 1706.3(2) | $[dHex]_1[Hex]_4[HexNAc]_6[NeuAc]_1$ | 2321.9 | 2321.9 |
| T4 | V69-K78 (1106.62) | N74 | 32.1 | 1563.7(2) | $[dHex]_1[Hex]_6[HexNAc]_3[NeuAc]_1$ | 2036.8 | 2036.7 |
| | | | 32.1 | 1482.7(2) | $[dHex]_1[Hex]_5[HexNAc]_3[NeuAc]_1$ | 1874.7 | 1874.7 |
| | | | 32.1 | 1584.2(2) | $[dHex]_1[Hex]_5[HexNAc]_4[NeuAc]_1$ | 2077.8 | 2077.8 |

[a] Monoisotopic mass value.

ラット脳のThy-1のN-結合型糖鎖については，これまでに抗体カラム等を用いて精製されたThy-1をトリプシン消化後，糖ペプチドごとに糖鎖を切り出し，ゲルろ過や，エキソグリコシダーゼ消化等を用いて分析した例が報告されている．Asn23には，高マンノース型（M5，6）が，Asn74には，コアがフコシル化された複合型糖鎖と，マイナー糖鎖としてハイブリッド型糖鎖及び高マンノース型糖鎖が結合していることが明らかにされているが[16,17]，電気泳動とLC/MS/MSを組み合わせることによって，微量の膜タンパク質を，抗体を使用せずに簡便且つより詳細に解析できることがわかる．尚，Asn98に結合する糖鎖及びGPIアンカーについては，トリプシン消化によって得られた糖ペプチドの親水性が高く，LCカラムに保持されなかったため，他の酵素消化によって得られた糖ペプチドを解析することによって明らかにしている（データ省略）．

以上のように，LC/MS/MSによるペプチド・糖ペプチドマッピングにおいて，糖鎖に特徴的なオキソニウムイオンを用いて糖ペプチドのプロダクトイオンスペクトルを取り出す方法は，タンパク質を同定すると同時に，糖鎖結合部位を決定し，結合部位ごとの糖鎖構造を推定することを可能にする．2次元HPLCとの組み合わせや，2次元電気泳動で分離された糖タンパク質の解析も可能であることから，今後，グライコプロテオミクスの分野で役立つことが期待される．

## 文　献


1) Varki A. Biological roles of oligosaccharides: all of the theories are correct. Glycobiology 1993;3:97–130.
2) Dennis JW, Granovsky M, Warren CE. Glycoprotein glycosylation and cancer progression. Biochim Biophys Acta 1999;1473:21–34.
3) Sato Y, Kimura M, Yasuda C, Nakano Y, Tomita M, Kobata A, Endo T. Evidence for the presence of major peripheral myelin glycoprotein P0 in mammalian spinal cord and a change of its glycosylation state during aging. Glycobiology 1999;9:655–660.
4) Ohta M, Kawasaki N, Hyuga S, Hyuga M, Hayakawa T. Selective glycopeptide mapping of erythropoietin by on-line high-performance liquid chromatography—electrospray ionization mass spectrometry. J Chromatogr A 2001;910:1–11.
5) Hirabayashi J, Arata Y, Kasai K. Glycome project: concept, strategy and preliminary application to Caenorhabditis elegans. Proteomics 2001;1:295–303.
6) Sullivan B, Addona TA, Carr SA. Selective detection of glycopeptides on ion trap mass spectrometers. Anal Chem 2004;76:3112–3118.
7) Carr SA, Huddleston MJ, Bean MF. Selective identification and differentiation of N- and O-linked oligosaccharides in glycoproteins by liquid chromatography-mass spectrometry. Protein Sci 1993;2:183–196.
8) Huddleston MJ, Bean MF, Carr SA. Collisional fragmentation of glycopeptides by electrospray ionization LC/MS and LC/MS/MS: methods for selective detection of glycopeptides in protein digests. Anal Chem 1993;65:877–884.
9) Nemeth JF, Hochgesang GP Jr, Marnett LJ, Caprioli RM, Hochensang GP Jr. Characterization of the glycosylation sites in cyclooxygenase-2 using mass spectrometry. Biochemistry 2001;40:3109–3116.
10) Harazono A, Kawasaki N, Kawanishi T, Hayakawa T. Site-specific glycosylation analysis of human apolipoprotein B100 using high-performance liquid chromatography/electrospray ionaization tandem mass spectrometry. Glycobilogy in press.
11) Durand G, Seta N. Protein glycosylation and diseases: blood and urinary oligosaccharides as markers for diagnosis and therapeutic monitoring. Clin Chem 2000;46:795–805.
12) Aoyagi Y. Carbohydrate-based measurements on alpha-fetoprotein in the early diagnosis of hepatocellular carcinoma. Glycoconj J 1995;12:194–199.
13) Aoyagi Y, Isokawa O, Suda T, Watanabe M, Suzuki Y, Asakura H. The fucosylation index of alpha-fetoprotein as a possible prognostic indicator for patients with hepatocellular carcinoma. Cancer 1998;83:2076–2082.
14) Yamashita K, Taketa K, Nishi S, Fukushima K, Ohkura T. Sugar chains of human cord serum alpha-fetoprotein: characteristics of N-linked sugar chains of glycoproteins produced in human liver and hepatocellular carcinomas. Cancer Res 1993;53:2970–2975.
15) Schachner M, Martini R. Glycans and the modulation of neural-recognition molecule function. Trends Neurosci 1995;18:183–191.
16) Parekh RB, Tse AG, Dwek RA, Williams AF, Rademacher TW. Tissue-specific N-glycosylation, site-specific oligosaccharide patterns and lentil lectin recognition of rat Thy-1. Embo J 1987;6:1233–1244.
17) Williams AF, Parekh RB, Wing DR, Willis AC, Barclay AN, Dalchau R, Fabre JW, Dwek RA, Rademacher TW. Comparative analysis of the N-glycans of rat, mouse and human Thy-1. Site-specific oligosaccharide patterns of neural Thy-1, a member of the immunoglobulin superfamily. Glycobiology 1993;3:339–348.


## 要　約


LC/MS/MSは，アミノ酸配列情報に加え，糖鎖構造に関する情報についても得ることができ，糖ペプチドの解析にも有用である．QqTOF-MSを用いたLC/MS/MSは，糖ペプチドのピークを特定し，ペプチドを同定し，結合糖鎖構造に関する情報も得ることができる．本稿では，糖ペプチドの解析例として，APF及び電気泳動で分離されたGPIアンカー型タンパク質の解析例を示す．